THE GEOLOGICAL SOCIETY OF AMERICA®

Multiproxy lacustrine records of post-glacial environmental change from the Uinta Mountains, Utah, USA

Jeffrey S. Munroe[1,†] and Benjamin J.C. Laabs[2]
[1]*Geology Department, Middlebury College, Middlebury, Vermont 05753, USA*
[2]*Department of Geosciences, North Dakota State University, Fargo, North Dakota 58108, USA*

ABSTRACT

Twenty-one sediment cores were obtained from 20 lakes in the Uinta Mountains, Utah, USA. Depth-age models were developed using ^{14}C dating, and sediments were analyzed for loss-on-ignition (LOI), carbon-nitrogen ratio (C:N), and grain size distribution. Although some of these cores have been considered individually in previous studies, here the entire set of cores is evaluated collectively to identify consistent patterns, commonalities, and trends in the post-glacial interval. All lakes accumulated substantially greater amounts of submicron-size clastic material before ca. 9.5 ka BP. This pattern is interpreted as a signal of prolonged landscape instability following deglaciation. Values of LOI and C:N exhibit a strong, positive correlation in nearly all lakes, indicating that organic matter accumulation is controlled by the influx of terrestrial material. In the six lakes exhibiting the strongest correlation, and featuring the most robust inflowing streams, median grain size and the abundance of sand increased between 10 and 6 ka BP, simultaneous with increases in LOI and C:N. This correspondence is interpreted as evidence for frequent high-intensity storms during the early Holocene, likely driven by enhanced monsoonal circulation. The early parts of five of the records contain a sharp increase in LOI. Lakes exhibiting this pattern are typically smaller and shallower, and are located in less rugged watersheds. Finally, all six cores from the western Uinta Mountains contain evidence for an environmental perturbation ca. 4.5 ka BP. Although the nature of this event is unclear, these lakes accumulated notably finer-grained sediment with less organic matter at this time. This analysis illuminates the post-glacial history of this strategically located mountain range, and underscores the value inherent in analyzing cores from multiple lakes when reconstructing paleoclimatic history.

†jmunroe@middlebury.edu

INTRODUCTION

Lacustrine sedimentary archives are invaluable records of environmental change. Numerous physical, chemical, and biological properties of lake sediments can be evaluated in the laboratory and serve as proxies for past environmental conditions. Some of these proxies are equivocal in isolation, but when combined in a multiproxy approach they can support nuanced paleoenvironmental reconstructions (e.g., Birks and Birks, 2006; Anderson et al., 2015). Furthermore, the presence of organic matter suitable for radiocarbon dating in most late Quaternary lake sediments allows interpretation of multiproxy records as time series tracking the evolution of environmental conditions within a lake and in the surrounding watershed. This basic strategy forms the foundation for all paleolimnological investigations (Cohen, 2003).

Paleolimnological records have revealed significant details about post-glacial environmental change in the Rocky Mountains. To provide just a few examples, transects of cores extending from shallow to deep water (Shuman et al., 2009, 2015; Shuman and Serravezza, 2017), along with stable isotope records from lacustrine carbonates (Anderson, 2011), have documented hydroclimate variability and corresponding lake-level fluctuations. Numerous studies have quantified charcoal abundance as a source of information about past fire regimes (Millspaugh et al., 2000; e.g., Whitlock and Larsen, 2002; Power et al., 2011). Shifts in diatom and pollen assemblages over time have been interpreted as signals of changes in water chemistry (Saros et al., 2003; Wolfe et al., 2003; Moser et al., 2010) and vegetation communities (Fall, 1988; Reasoner and Jodry, 2000), respectively. Variations in the mineralogy and geochemistry of lake sediments have shed light on past changes in dust flux and paleoaridity (Routson et al., 2016), and have revealed the degree to which human activity has affected dust deposition in this region (Neff et al., 2008; Moser et al., 2010).

Despite the abundance of paleolimnological studies in the Rocky Mountains, numerous questions remain about post-glacial paleoclimate and environmental change in the region. For instance, the extent and timing of cirque glaciation during the Holocene has been the target of long-running interest (e.g., Davis et al., 2009). However, although Neoglacial records from some areas have been well constrained (Munroe et al., 2012), the history of Holocene glaciation (if any occurred) in other parts of the Rocky Mountains remains unclear and open to revision (e.g., Dahms et al., 2018). Similarly, the regional pattern of lake level change is complicated, likely reflecting shifting boundary conditions as the Laurentide Ice Sheet retreated toward its final demise (Shuman et al., 2015; Shuman and Serravezza, 2017). At the same time, changes accompanying evolution of the modern North America Monsoon system may have altered the balance of precipitation between winter and summer seasons (e.g., Whitlock and Bartlein, 1993), likely contributing to variability in hydrology (e.g., Shuman et al., 2010), snowpack (e.g., Anderson, 2012), and fire regimes (e.g., Millspaugh et al., 2000; Frechette and Meyer, 2009). Given their inherently interdisciplinary nature, and the well-dated time series that can be generated from sediment cores, paleolimnological investigations are well suited to address these and other questions about how Rocky Mountain environments evolved during the immediate post-glacial period and ensuing Holocene.

At the start of any paleolimnology study, a decision must be made about how many lakes will be considered and how many cores will be analyzed from each lake. Although a subset of paleolimnological investigations has strongly demonstrated the added interpretive potential provided by analyzing multiple cores (e.g., Digerfeldt, 1986; Abbott et al., 2000; Shuman et al., 2009, 2010), most studies continue to rely on a single core, usually collected from deep water near the lake center. Similarly, although compilations of records from multiple lakes have been used as sources of information about regional patterns of environmental change (e.g., Street and Grove, 1979; Carter et al., 2013;

GSA Bulletin; January/February 2020; v. 132; no. 1/2; p. 48–64; https://doi.org/10.1130/B35056.1; 14 figures; 3 tables; Data Repository item 2019191; published online 2 May 2019.

Shuman and Serravezza, 2017), most studies rely on a single lake, or a small number of lakes, to represent a relatively large surrounding area.

This project employed an intentionally different approach: collecting cores from a large number of lakes in a geographically restricted area. These cores were analyzed for a consistent series of physical proxies, and these records were converted to time series supported by radiocarbon-based age models. The entire group of time series was then considered holistically with the goal of determining what patterns, commonalities, and trends would emerge from examination of such a large data set. This approach was designed to allow the identification of signals of environmental variability that might be overlooked or misinterpreted in an analysis of a smaller number of cores.

The sediment cores analyzed in this project were obtained from lakes in the Uinta Mountains of northeastern Utah. These mountains occupy a strategic location for studying the evolution of post-glacial climate in the western U.S. They lie along the boundary between the monsoonal circulation in the southwestern U.S and the area dominated by Pacific high pressure during the summer (Mock, 1996). They also parallel the prevailing storm track followed by Pacific storms penetrating inland during winter months (Mitchell, 1976). Topographically, they are the highest mountains between the Colorado Rocky Mountains and the Sierra Nevada, and serve as significant headwaters for both the Green/Colorado River and the Great Salt Lake (Jeppson et al., 1968; Jacoby, 1975). Ecologically, they represent a significant transition zone between floral and faunal assemblages dominant in areas farther to the south and north (Shaw and Long, 2007).

Sediment cores were collected from lakes in the Uinta Mountains as part of a project focused on the spatial and temporal pattern of the Last Glacial Maximum in this range (Munroe et al., 2006; Laabs et al., 2009). Previous work on these cores has revealed considerable information about the post-glacial evolution of these mountains. For instance, sedimentary records downstream from rock glaciers have yielded a record of Holocene periglacial activity (Munroe et al., 2013). Basal radiocarbon ages from these lakes, combined with cosmogenic surface-exposure ages for downvalley moraines, have constrained the timing and pace of deglaciation after the Last Glacial Maximum (Munroe and Laabs, 2017). Comparison of multi-proxy records has demonstrated that adjacent lakes can preserve strongly contrasting records depending on their hydrogeomorphic setting (Corbett and Munroe, 2010). Watershed controls on the abundance of lacustrine organic matter, as revealed by the commonly employed "loss-on-ignition" proxy, have been deduced through statistical inter-comparison of lake and watershed properties (Munroe, 2007a, 2019). In previous and ongoing work, geochemical time series through these cores are being interpreted as signals of changing eolian dust delivery (e.g., O'Keefe et al., 2016a, 2016b). All of these studies, however, focused on just one or two cores, or on single proxies in a number of lakes.

This study reported here is the first to focus collectively on the entire Uinta lake data set. The central objective is to consider multiproxy records from a large number of lakes simultaneously in order to identify and interpret post-glacial environmental changes. Significantly, because previous work has already explored some of the details revealed by focused study of subsets of these cores, the emphasis here is on what can be learned through integration of multiple records. The primary proxies utilized—loss-on-ignition, carbon-nitrogen ratio, and grain size distribution—are commonly employed in paleolimnological studies. However, the large number of lakes cored in a relatively concentrated area is unusual and supports a diverse array of insights into latest Pleistocene and Holocene environmental changes in the Uinta Mountain region.

SETTING

The Uinta Mountains are a prominent component of the Rocky Mountain system in the western United States (Fig. 1). Located in northeastern Utah, the Uinta Mountains (hereafter, the "Uintas") extend along an east-west axis for ~200 km parallel to the Utah-Wyoming border. Bedrock of the Uintas is a thick sequence of Precambrian quartzite, sandstone, and argillite that was uplifted as a doubly plunging anticline during the Laramide Orogeny (Bradley, 1936; Sears et al., 1982; Dehler et al., 2007). The axis of this anticline roughly coincides with the main east-west ridgeline of the mountains. As a result, bedding dips northward along the north flank of the Uintas, and southward along the south flank. Summit elevations reach a maximum of 4123 m above sea level (asl) at Kings Peak, the highest mountain in Utah.

No glaciers remain in the Uintas today, but the landscape exhibits classic examples of alpine glacial geomorphology testifying to the presence of more than 2000 km^2 of active glacial ice during the Last Glacial Maximum (Munroe and Laabs, 2009). Most of these glaciers, which were up to 40 km long, were confined to individual valleys (Laabs and Carson, 2005; Munroe, 2005), but several glaciers in the western Uintas coalesced to form an icefield that locally inundated the topography (Refsnider et al., 2008). Cosmogenic ^{10}Be surface-exposure dating indicates that these glaciers began to retreat around 18,000 years ago (Munroe et al., 2006; Laabs et al., 2009). Small glaciers may have occupied some sheltered cirques during the Younger Dryas stade in the latest Pleistocene (Munroe and Laabs, 2017), whereas periglacial activity, including rock glacier formation, dominated the Holocene (Munroe, 2002; Munroe et al., 2013).

Lakes are abundant in the higher elevation landscapes of the Uintas, particularly within the area covered by active ice during the last glaciation. Many lakes occupy basins eroded by

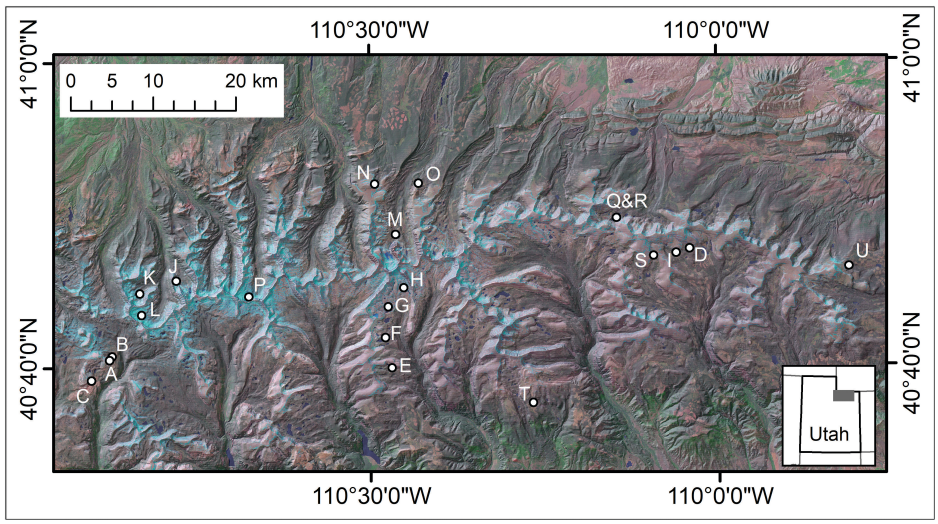

Figure 1. Lakes cored in the Uinta Mountains for this project, with letters keyed to Table 1, displayed over a shaded Landsat image. Inset shows the location of the Uinta Mountains in northeastern Utah, USA.

TABLE 1. LOCATIONS AND DIMENSIONS OF UINTA MOUNTAIN LAKE CORES, UTAH, USA

Fig. 1 code	Lake ID	Lake name	Latitude (°N) (DD MM.mmm)	Longitude (°W) (DD MM.mmm)	Elevation (m)	Water depth (m)	Lake area (ha)	A_W/A_L*	Core length (cm)	Penetrated to Inorganic?
A	04-01	Marshall	40° 40.538	110° 52.452	3043	10.7	8.0	7.5	190	Yes
B	04-02	Hoover	40° 40.824	110° 50.824	3018	7.9	7.8	17.8	156	Yes
C	04-03	Pyramid	40° 39.192	110° 54.094	2957	10.7	5.8	13.3	180	No
D	04-04	Elbow	40° 47.619	110° 02.502	3326	10.7	10.0	33.5	217	Yes
E	04-06	Swasey	40° 40.048	110° 28.000	3267	9.5	14.6	21.7	198	Yes
F	04-07	Spider	40° 42.019	110° 28.756	3316	12.8	8.1	44.8	324	Yes
G	04-08	Little Superior	40° 44.003	110° 28.461	3417	9.5	6.0	51.8	264	Yes
H	04-09	North Star	40° 45.195	110° 27.075	3474	5.8	5.8	49.7	198	Yes
I	05-01	Reader	40° 47.445	110° 03.583	3341	4.0	4.8	11.3	246	Yes
J	05-02	Ostler	40° 45.579	110° 46.749	3218	5.2	5.3	21.9	213	Yes
K	05-03	Kermsuh	40° 44.876	110° 49.926	3145	5.2	3.9	68.2	219	Yes
L	05-04	Ryder	40° 43.540	110° 49.688	3243	17.4	8.6	17.3	347	Yes
M	05-05	Lower Red Castle	40° 48.793	110° 27.762	3279	9.1	17.6	65.8	142	Yes
N	05-06	Bald	40° 52.030	110° 29.540	3367	7.0	2.2	14.5	355	Yes
O	05-07	Hessie	40° 52.102	110° 25.742	3237	6.1	5.3	7.5	258	No
P	05-08	Deadhorse	40° 44.711	110° 40.381	3316	12.5	5.8	12.8	199	Yes
Q	05-09d	Island	40° 49.796	110° 08.684	3285	11.4	45.3	24.1	308	Yes
R	05-09e	Island	40° 49.612	110° 08.934	3285	9.9	45.3	24.1	327	Yes
S	05-10	Taylor	40° 47.193	110° 05.478	3421	11.0	9.0	35.4	270	Yes
T	06-01	Upper Lily Pad	40° 37.665	110° 15.993	3129	9.8	4.0	76.3	371	Yes
U	98-01	Hacking	40° 43.150	109° 43.057	3239	4.3	3.4	38.8	259	Yes

*Ratio of watershed area to lake area.

Pleistocene glaciers, or dammed by moraines and other deposits of glacial sediment (Atwood, 1908, 1909). These lakes, which range in area from <1 to more than 70 ha, are surrounded by a variety of vegetation communities (Shaw and Long, 2007; Munroe, 2012). Intermediate elevations feature a monoculture of *Pinus contorta* (Lodgepole Pine), whereas *Picea engelmannii* (Engelmann spruce) and *Abies lasiocarpa* (Subalpine fir) dominate the upper-subalpine forests. Lakes in forest openings are bordered by meadows with common species including *Danthonia intermedia* (wild oat grass), *Deschampsia caespitosa* (tufted hairgrass), and *Carex scirpodiea* (single spike sedge). Landscapes above ~3300 m asl are mantled by alpine tundra featuring abundant forbs including *Acomastylis rossii* (Alpine avens) and *Polygonum bistortoides* (alpine bistort).

The climate of the Uintas is characterized by long, snowy winters and relatively cool summers. An extensive network of snowpack telemetry stations reveals that mean annual precipitation ranges from 500 to 925 mm, with more than 60% falling as snow at elevations >3300 m asl (Munroe and Mickelson, 2002; Munroe, 2003). Annual precipitation amounts are generally greatest at the western end of the range and decrease eastward (Munroe and Mickelson, 2002; Munroe et al., 2006; Laabs et al., 2009). Convective storm activity is common in the summer months, particularly at the eastern end of the range (Munroe, 2003). A remote automated weather station (Chepeta station) on the main Uinta ridgecrest at an elevation of 3705 m asl, along with temperature datalogger deployments in soil pedons, confirm that the mean annual temperature above ~3100 m asl is <0 °C (Munroe, 2006, 2007b; Bockheim and Munroe, 2014). Under these conditions, all of the lakes in this study freeze over in the winter, with a duration of ice cover extending roughly from October through June.

METHODS

Field Methods

Twenty lakes were cored in this project, evenly divided between the north and south slopes of the Uinta Mountain range (Fig. 1). Lakes were selected on the basis of their location, elevation, reported depth, setting, and accessibility for pack animals necessary for transporting equipment. Most lakes are grouped into six clusters, representing the headwaters of drainages where downvalley terminal moraines were dated with ^{10}Be cosmogenic surface-exposure dating (Munroe et al., 2006; Laabs et al., 2009). The lakes range from 2957 to 3474 m asl in elevation and have an average surface area of 9.1 ha (Table 1). The average watershed is ~30× larger than the corresponding lake surface, with an order-of-magnitude range from 7.5 to 76.3×. Most lakes are surrounded by upper-subalpine forest of *Picea engelmannii* (Engelmann spruce) and *Abies lasiocarpa* (Subalpine fir). However, the extent of tundra in the watershed becomes increasingly significant for lakes at higher elevations (Fig. DR1[1]), and the watershed for the highest lake (04-09) is located almost entirely above treeline.

All but one of the lakes were cored from a floating platform designed and built at Middlebury College, Middlebury, Vermont, USA (Fig. DR2; see footnote 1). Before coring, a bathymetric survey was conducted with a GPS-enabled sonar device, and the perimeter of each lake was explored on foot. Information from this survey was used to select a coring location in deep water near the lake center, far from prominent inlets or steep slopes (terrestrial and subaqueous) that could deliver sediment through mass wasting. A modified Reasoner-type percussion corer (Reasoner, 1993) fitted with a piston, metal nose cone with integrated core catcher, and ~30 kg driving weight was used to collect sediment in a 6-m-long barrel of 7.5-cm-diameter PVC pipe. Driving of the percussion corer began at the sediment-water interface, but it was not possible to retrieve the unconsolidated near-surface sediment with this technique. As a result, all cores were artificially truncated at a depth of ~50 cm. After driving to the point of refusal, the core barrels were extracted using a hand-operated winch. Cores were cut to ~80 cm lengths with a hacksaw, capped, and transported by pack animals before shipping. After arrival in the lab, all core sections were stored at 4 °C until processing.

One lake, (98-01), was cored with a 2.5-cm-diameter Livingstone corer (Livingstone, 1955) through a 20-cm-diameter hole drilled through winter ice cover. Prior to coring, a grid of holes was drilled over the deeper end of the lake basin as identified on aerial imagery. A sounding weight was used to determine the bathymetry and select the coring location. The sedimentary sequence was collected in four successive drives, each of which was wrapped in saran and aluminum foil. Wrapped cores resulting from these drives were transported in capped lengths of 5-cm-diameter PVC pipe.

[1]GSA Data Repository item 2019191, Figures DR1–DR25, Tables DR1–DR3, and a database of measurements made on the Uinta lake cores, is available at http://www.geosociety.org/datarepository/2019 or by request to editing@geosociety.org.

Analytical Methods

Percussion cores were opened by slicing the PVC on both sides lengthwise with a circular saw and pulling a thin wire through the sediment from top to bottom. The Livingstone core drives were unwrapped and cut lengthwise with a knife. All cores were photographed and described before sampling. One half of each core section was wet-sieved to 500 µm at 1 cm intervals to separate organic material suitable for ^{14}C dating. These organic fragments were washed in distilled water, photographed under magnification, and identified when possible.

The other half of each percussion core was sampled in quadruplicate at 1 cm intervals using 10 ml plunger-type syringes with the end removed. Sample volumes averaged ~5 cm^3. The other half of each Livingstone core drive was divided into thirds for analysis. All samples were stored in labeled, 12 ml snap-cap vials. One sample from each cm in the percussion cores was stored at 4 °C as an archive. Samples from the Livingstone core were not archived.

Three samples from each cm were analyzed for a consistent set of physical and chemical properties. One sample was consumed during quantification of water content and loss-on-ignition at 550 °C with a Leco TGA 701 thermogravimetric analyzer (Munroe, 2007a, 2019). Water content, which reflects bulk density (Menounos, 1997), was determined from the mass lost during heating to 105 °C under a full nitrogen atmosphere for 4 h. Loss-on-ignition, considered a proxy for organic matter content (Dean, 1974), was calculated from the mass lost from this dried sample over 3 h at 550 °C under ambient atmosphere. Replicate analyses indicate that measurements with this technique are reproducible to within 1%.

Another sample from each cm was freeze-dried, ground to a fine powder, and analyzed in a Thermo Flash 2000 elemental analyzer to determine the abundance of carbon and nitrogen. The analyzer was calibrated with aspartic acid, and standard reference materials were analyzed every ~30 samples. Replicate analyses indicate that this method has a precision of ~1% for C and ~0.5% for N. No detectable change was observed in values after a subset of samples was acidified and reanalyzed, thus all carbon in these samples is inferred to be organic.

The fourth sample from each cm was analyzed for grain size distribution through laser scattering in a Horiba LA-950 with a 30-position autosampler. Pretreatments included 35% H_2O_2 (three additions of 10 ml over 7–10 days) to remove organic matter, and 0.1M NaOH (1 h at 85 °C) to remove biogenic silica. Sodium hexametaphosphate (3%) was used as a dispersant and all samples were physically mixed and sonified immediately prior to analysis. The Horiba LA-950 has an effective range from 10 nm to 3 mm, and a refractive index of 1.54 with an imaginary component of 0.1i was used in calculating the grain size distribution on a volume basis. Ten percent of the samples were automatically rerun as duplicates, along with selected samples exhibiting unusual grain size distributions relative to adjacent samples.

A subset of the archived samples, including all samples from cores 04-04 and 05-01, were analyzed for biogenic silica (bSi) content. These samples were freeze-dried and ground, and bSi was quantified through sequential extraction while leaching in 0.1M NaOH for 5 h at 85 °C (DeMaster, 1981). Dissolved Si content was determined for each aliquot by spectrophotometry at 812 nm after addition of reagents for a molybdate blue reaction (Strickland and Parsons, 1965). The %bSi was calculated from the y-intercept of a linear function fit to the results for extractions for hours 2 through 5. Analysis of replicates indicates that this method has a reproducibility of 10%.

Radiocarbon Dating and Depth-Age Modeling

Age control for the lake cores from the Uinta Mountains was provided by accelerator mass spectrometry (AMS) radiocarbon dating. Although the lack of carbonate bedrock in the Uintas greatly reduces the possibility of an old-carbon effect (MacDonald et al., 1991), dating of terrestrial organic material was preferred whenever possible. Terrestrial material isolated from the cores included conifer needles and cones, small wood fragments and twigs, and macroscopic charcoal. Concentrated pollen (1–20 mg, >90% *Pinus*) was used to date some sediments (Brown et al., 1989; Mensing and Southon, 1999). Layers dominated by *Daphnia* ephippia were also common in the deeper sediment of many lakes. When concentrated, these provided sufficient carbon for AMS dating. Concentrations of unidentified organics were dated in some situations when larger terrestrial organic fragments were not available. Finally, four samples of organic-rich bulk sediment were dated. Three of these came from deep sediment lacking macroscopic organic material. In the fourth instance, bulk sediment from a stratigraphically higher position was dated along with a conifer needle from the same depth to test the assumption that these lakes are free from an old-carbon effect.

Radiocarbon results were calibrated with the Intcal13 calibration curve (Reimer et al., 2013) and used along with their stratigraphic depths to construct depth-age models in the program CLAM (Blaauw, 2010). In some cases, additional age control was provided by matching prominent LOI excursions in one core with analogous excursions in a core from a nearby lake. In two cores (05-09e and 05-10), stratigraphic depths of individual radiocarbon dates were adjusted upward to accommodate the removal of prominent graded beds, inferred to have been deposited as an instantaneous events. Preferred age models utilized a smooth spline with a smoothing level of 0.1–0.2, an interval of 0.5 cm, and 1000 iterations per model. In two lakes (05-05, 05-07), only a linear depth-age model was possible because the number of radiocarbon dates was too small to support a spline. Although an effort was made to date organic matter from as close to the top and bottom of each core as possible, extrapolation in CLAM was still necessary to extend some age models.

Statistical Analysis

The analyses conducted on these cores generated a large volume of individual proxy measurements. To aid interpretation of these results, typical data reduction strategies and statistical tests were employed. These included Z-score transformation to normalize data to the standard deviation and mean of a specific proxy time series, interpolation to realign irregularly spaced time series, and non-parametric (Mann-Whitney, Spearman rank correlation) tests to evaluate differences and correlations between pairs of data sets. For clarity, details of these steps are presented in the appropriate sections of the discussion that follows.

RESULTS

Lacustrine Sediment Cores

A total of 21 sediment cores were retrieved and analyzed in this project, from 20 lakes (Fig. 1; Table 1). Coring at an additional lake (04-05) was attempted, but due to deep water (>20 m) and high winds, only a short core (63 cm) was retrieved and was not included in subsequent analyses. In lake 05-09, two cores (05-09d and 05-09e) were retrieved from deep basins on either side of a prominent end moraine that locally rises above the water surface.

The retrieved cores range in length from 142 to 371 cm and were obtained from water depths between 4.0 and 17.4 m (Table 1). The upper parts of most cores are massive gyttja with colors ranging from black (i.e., 10YR 2/1) to pinkish (i.e., 2.5YR 5/3) depending on the amount of organic matter present to disguise the typically reddish tones of clastic sediment derived from the Uinta bedrock. The upper parts of some cores are moderately vesicular with gas bubbles. Interme-

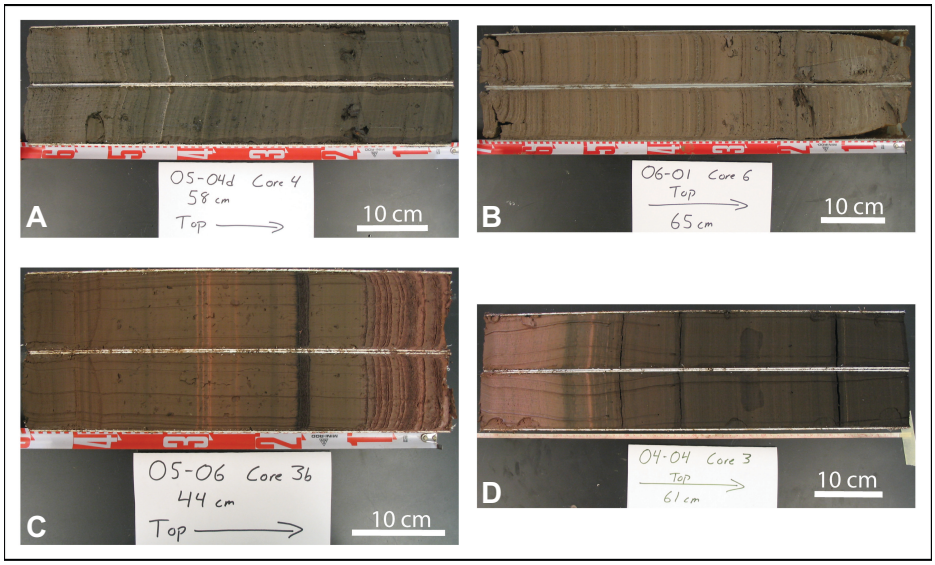

Figure 2. Representative photographs of sediment cores from Uinta Mountain lakes, Utah, USA. In all photographs the core name (i.e., "05-04d") is keyed to Table 1. The second designation, i.e., "Core 4", designates the core section. The length of each section in cm is noted, and the upward direction is indicated.

diate and lower sections are typically laminated at mm- to cm-scale (Fig. 2). Centimeter-thick bands of finer grained, often reddish or gray, sediment are also common. Cores 05-09e and 05-10 included a prominent graded bed ~10 cm thick. The bottom parts of these beds are 30%–50% sand that grade upward to silt capped by clay. These layers contain notably less dispersed organic matter than the sediment immediately above and below them, yet they often contain larger fragments of wood and other terrestrial organic debris. Nearly all cores penetrated into inorganic sediment that accumulated before the onset of organic productivity in the lake and watershed. Basal sediments feature alternating layers of relatively coarse sand and dense clay that are devoid of macroscopic organic matter.

Radiocarbon Ages and Depth-Age Modeling

A total of 133 radiocarbon analyses were completed on organic materials isolated from the Uinta Mountain lake cores (Table DR1). The youngest core-top ages range from 500 to 1000 ^{14}C years, confirming that the uppermost, unconsolidated sediment was not retrieved by percussion coring. The oldest age is 15,350 ^{14}C years, from the base of core 04-06. Bulk sediment and a conifer needle from the same depth (47 cm) in core 04-01 yielded similar ages of 3615 ± 42 and 3464 ± 39 ^{14}C years, respectively, supporting the assumption that lakes in the quartzite terrane of the Uintas are not influenced by a hard water effect. Radiocarbon analyses on *Daphnia* ephippia and pollen samples from the same depth in three cores (05-01, 05-06, and 05-09e) also returned similar results (Table DR1). In contrast, paired analyses in cores 04-04, 05-02, 05-04, and 05-10 failed to match.

All of the radiocarbon ages were successfully calibrated with the Intcal13 curve (Table DR1). When plotted as depth versus age, the majority of these fall along prominent, nearly linear trends (Fig. 3; Figs. DR3–DR24; see footnote 1). Nonetheless, 21 of the 133 ages (16%) were ignored in construction of the depth-age models. Some were ignored because they plot as obvious outliers in depth-age space, for example, the results from

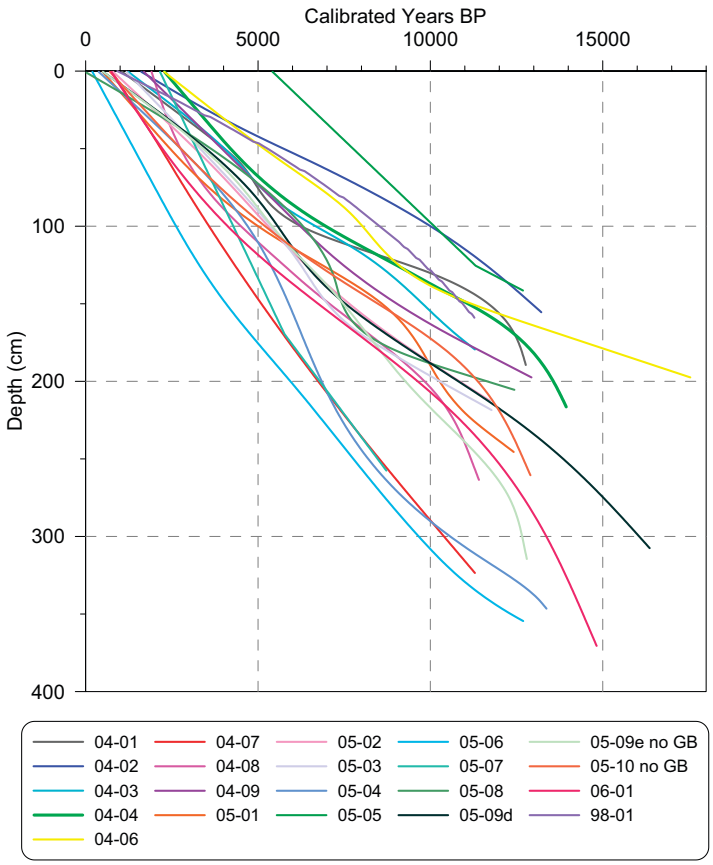

Figure 3. Depth-age models for the Uinta lake cores, Utah, USA, determined in the program CLAM (Blaauw, 2010). In two cores (05-09e and 05-10), stratigraphic depths of some radiocarbon dates were adjusted upward before age modeling to accommodate the removal of prominent graded beds ("no GB"), inferred to have been deposited as instantaneous events. Preferred age models utilized a smooth spline with a smoothing level of 0.1–0.2, an interval of 0.5 cm, and 1000 iterations per model. In two lakes (05-05, 05-07), only a linear depth-age model was possible because the number of radiocarbon dates was too small to support a spline. All cores were truncated below the sediment-water interface because loose sediment could not be retrieved with the percussion corer.

216 to 217 cm in core 05-04, from 68 to 69 cm in core 05-09e, and sample HL-625 from core 98-01 (Table DR1; Figs. DR3–DR24). Others require stratigraphic reversals for which there is no sedimentary evidence. Most of the ignored ages were determined on pollen and daphnia concentrates from deep, inorganic sediments. Some of these ages, for instance from the bases of cores 04-06, 04-08 and 05-10, are ignored because they are older than the basal ages for neighboring lakes and are inconsistent with cosmogenic ^{10}Be ages determined for terminal moraines located more than 10 km downvalley (Laabs et al., 2009). Others, such as the age from the base of core 06-01 require unrealistic changes in sedimentation rate. Although precautions were taken, it is likely that these samples were contaminated by a source of older carbon during the process of concentrating pollen and *Daphnia* ephippia. It is important to note, however, that 75% of the ignored dates were within the bottom 10% of their respective cores, and 33% were within 3 cm of their ultimate core base. Decisions about whether or not to include these results in the depth-age models, therefore, do not influence the ages assigned to the stratigraphically higher sediments that are the focus of this analysis.

Most of the resulting depth-age models are supported by 5–7 radiocarbon ages (Table DR2). Two models (cores 05-05 and 05-07) are supported by just three radiocarbon ages; for these cores only a linear depth-age model is used. Selection of ages as close to the bottom and top of each core as possible reduced the necessary extrapolation in constructing depth-age models. Average upward extrapolation was 21 cm, whereas downward extrapolation was 8 cm. However, in 15 of the cores (71%), upward extrapolation was <20 cm, and in 66% of the cores the deepest age control is within 10 cm of the core base (Table DR2).

The error ranges between the minimum and maximum age estimates within each model are mostly <100 yrs, defining a narrow age window. Exceptions include the uppermost parts of cores 04-09 and 05-07, where considerable (>90 cm) extrapolation above the stratigraphically highest radiocarbon age was necessary (Figs. DR11 and DR18). Estimated sedimentation rates average 0.25 mm/yr. Core 05-07 had the highest mean sedimentation rate (0.41 mm/yr), whereas cores 04-02, 04-06, and 98-01 had mean rates ≤0.15 mm/yr (Fig. 4).

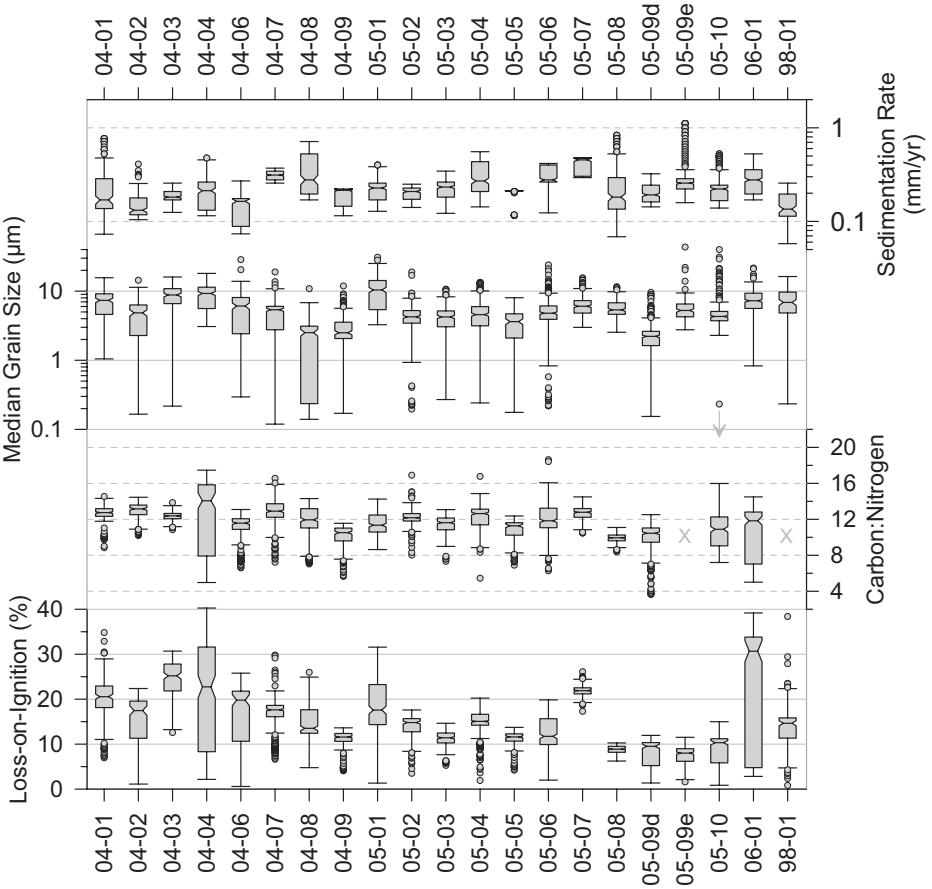

Figure 4. Boxplots of measured values in the Uinta Mountain lake sediment cores, Utah, USA. Core names along the bottom and top axes are keyed to Table 1. Boxes span the interquartile range, with a notch at the median. Whiskers extend to 1.5-times the interquartile range, and outliers are shown as circles. Loss-on-ignition was determined through thermogravimetric analysis. Carbon-nitrogen ratio was measured with an elemental analyzer. Median grain size was assessed with a laser scattering particle size analyzer. Sedimentation rate (in mm/yr) was calculated from the depth-age models (Fig. 3). Note that median grain size and sedimentation rate are displayed on logarithmic axes.

Analytical Results

A total of 5136 loss-on-ignition measurements were made on the 21 cores. The overall average LOI value is 14.7%, but there is considerable variation between the cores (Table 2; Figs. 4 and 5). Core 06-01 has the highest median value, ~30%. In contrast, Cores 05-08, 05-09d, and 05-09e have median values <10%. Some lakes in close proximity to one another, for instance 04-01, 04-02, and 04-03 (A–C in Fig. 1), exhibit a surprisingly wide range of LOI values. Other lakes situated along elevational transects (for instance 04-06 through 04-09, E–H in Fig. 1) exhibit decreasing median LOI with increasing elevation. Core 04-04 has the widest intra-lake range in LOI, from ~2% to 40% (Fig. 4). Nearly all cores penetrated through a deep transition into inorganic sediment. The exceptions are cores 04-03 and 05-07, which failed to reach this depth (Fig. 5). In some cores, for example 04-02, 05-01 and 05-06, and 06-01, this transition is quite sharp, occurring over <5 cm. In other cores, for example 04-04 and 04-09, this transition occurs over tens of cm. The sediment comprising core 05-08 is overall low in organic content, and no specific transition is obvious.

The data set includes 4568 individual C:N measurements. This total is lower than for LOI because C:N was not measured on cores 05-09e and 98-01, and because in some deep sediments the values of N fell below detection limits. Most C:N measurements cluster between 8 and 16, within an overall average of 11.6 (Figs. 4 and 6), reflecting a mixture of terrestrial and lacustrine organic matter (Meyers and Ishiwatari, 1993, 1995). In contrast to LOI, values of C:N are more consistent between neighboring lakes, for instance 04-01, 04-02, and 04-03 (A–C in Fig. 1). C:N is also generally lower in lakes with lower LOI, for example cores 05-08 and 05-09d. The highest C:N values (>16), reflecting pulses of terrestrial organic matter, are outliers in cores 05-02, 05-04, and 05-06 (Fig. 6).

TABLE 2. SUMMARY STATISTICS FOR PROXIES MEASURED IN THE UINTA MOUNTAIN LAKE CORES, UTAH, USA

	LOI						C:N						Median grain size					
Core Code	Mean (%)	Median (%)	Stdev (%)	Max (%)	Min (%)	n	Mean	Median	Stdev	Max	Min	n	Mean (μm)	Median (μm)	Stdev (μm)	Max (μm)	Min (μm)	n
04-01	10.4	20.6	5.2	38.7	7.0	191	12.6	12.7	1.1	14.6	8.9	185	6.9	7.3	3.0	15.6	1.0	191
04-02	14.9	17.5	5.9	22.4	1.1	156	12.9	13.2	1.0	14.5	10.2	143	4.5	4.9	3.1	14.4	0.2	156
04-03	24.3	25.2	4.3	30.7	12.6	180	12.3	12.4	0.5	13.9	10.9	179	8.2	8.8	3.8	16.0	0.2	180
04-04	21.8	22.8	11.1	40.3	2.2	217	12.8	14.1	3.7	17.5	5.0	215	8.8	9.3	3.5	18.1	3.1	218
04-06	16.4	19.8	7.5	25.8	0.6	198	10.9	11.6	1.8	13.1	6.6	174	5.7	6.1	3.8	28.6	0.3	193
04-07	16.7	17.6	3.7	29.8	6.7	324	12.8	12.9	1.5	16.6	7.2	324	4.6	5.4	2.7	18.9	0.1	324
04-08	14.7	13.5	4.8	26.0	4.8	264	11.7	11.9	1.9	14.3	7.0	263	2.3	2.5	1.8	10.9	0.1	264
04-09	10.8	11.6	2.4	13.6	4.1	198	10.0	10.5	1.4	11.6	5.6	198	2.8	2.5	1.9	11.9	0.2	198
05-01	18.3	17.6	5.6	31.6	1.3	246	11.6	11.3	1.3	14.3	8.6	246	10.4	10.4	5.3	31.0	3.3	244
05-02	14.0	14.8	2.6	17.6	3.5	213	12.2	12.2	1.0	16.9	8.0	213	4.4	4.3	2.0	19.0	0.2	213
05-03	11.3	11.4	1.9	14.6	5.3	219	11.4	11.6	1.0	13.1	7.3	219	4.3	4.2	1.7	10.7	0.3	219
05-04	14.9	15.1	3.0	20.2	1.9	347	12.3	12.6	1.3	16.8	5.4	347	4.9	4.6	2.5	13.4	0.2	347
05-05	10.9	11.6	2.2	13.7	4.2	142	10.7	11.3	1.4	12.4	6.9	142	3.3	3.6	1.9	8.0	0.2	142
05-06	11.8	11.7	4.3	19.9	2.0	355	12.0	11.8	1.7	18.6	6.3	355	5.4	4.8	2.9	24.0	0.2	355
05-07	21.9	21.9	1.2	26.1	17.3	258	12.7	12.8	0.7	14.5	10.5	258	6.4	6.0	2.3	15.6	3.0	248
05-08	8.8	8.9	0.8	10.3	6.3	211	9.9	9.9	0.5	11.1	8.4	194	5.8	5.5	1.7	11.6	2.5	211
05-09d	8.1	9.5	2.9	12.0	1.4	308	9.9	10.5	1.9	12.5	3.7	289	2.3	2.2	1.5	9.6	0.2	308
05-09e	7.6	8.1	2.0	11.5	2.5	314	--	--	--	--	--	--	5.5	5.2	1.6	13.9	2.8	159
05-10	8.8	10.4	3.3	15.0	0.9	261	10.6	10.7	1.7	14.2	7.2	253	5.2	4.3	3.9	40.1	2.3	257
06-01	22.4	30.7	13.6	39.2	2.8	371	10.4	11.8	2.9	14.5	5.0	371	7.6	7.3	2.7	21.7	0.8	371
98-01	13.7	14.6	5.0	38.4	0.8	163	--	--	--	--	--	--	7.2	6.9	3.5	16.3	0.2	129

Note: LOI—loss-on-ignition; C:N—carbon-nitrogen ratio; Stdev—standard deviation.

Grain size distributions were analyzed for 4927 samples (Figs. 4 and 7). This total is lower than the LOI measurements because grain size was measured at a 2 cm interval in core 05-09e. The overall average median grain size is 5.6 μm (very fine silt). Core 05-01 has the coarsest median grain size (~10 μm), whereas core 05-09d is considerably finer (2.3 μm). Some cores, notably 04-06, 05-06, 05-09e, and 05-10, contain numerous coarse outliers with median grain sizes up to 40 μm (coarse silt, Fig. 7). In contrast, core 04-04 contains numerous ~1-cm-thick layers rich in fine silt. Some cores record step change in median grain size, for instance at ca. 4.5 ka BP in core 05-04 (Fig. 7).

Many individual particle size distributions are strikingly bimodal, with a coarser mode of fine silt and a finer mode in the submicron (colloidal) range (Fig. 8). In some cores, the maximum abundance of submicron material (on a volume basis) exceeds 80% (Table 3). The average maximum abundance of submicron material in each core is 55%, and in all cores the maximum is greater than 23%. In contrast, the abundance of clay-sized (1–2 μm) material is rarely more than 20%, with an average of 6%.

DISCUSSION

Lacustrine Sediment Proxies

The three main proxies utilized in this study, LOI, C:N, and grain size distribution, are employed extensively in paleolimnological investigations. Loss-on-ignition, for instance, is well-established as a simple and reliable method for quantifying the organic content of sediments (e.g., Dean, 1974; Heiri et al., 2001; Munroe,

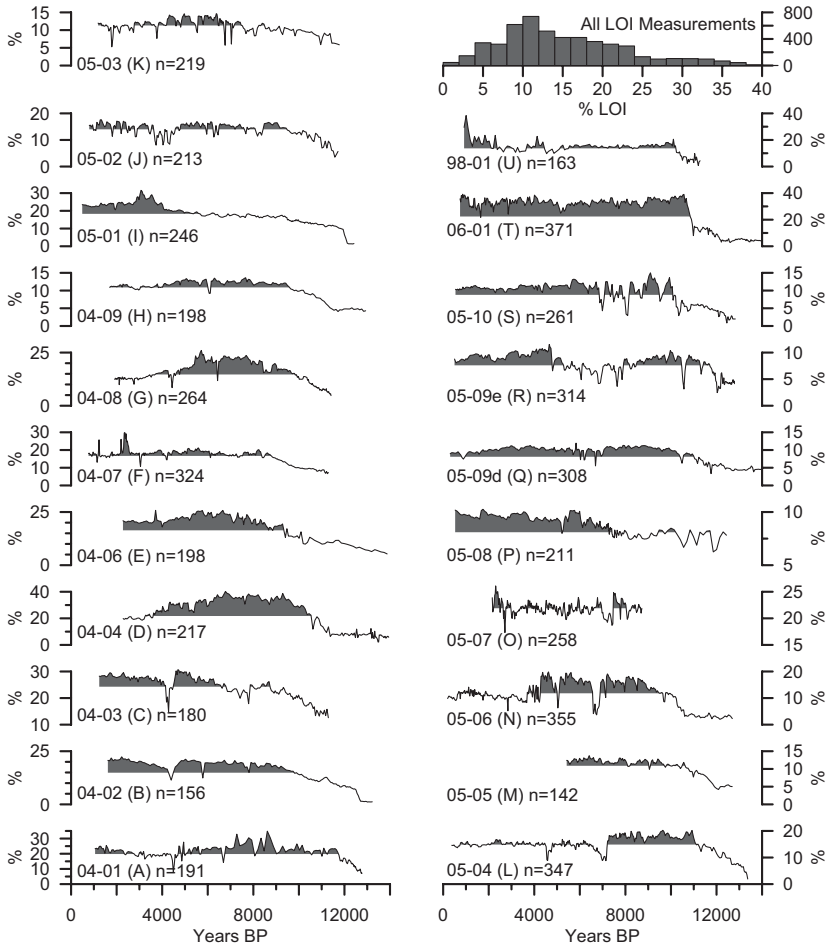

Figure 5. Time series of organic matter content measured at loss-on-ignition (%LOI) in Uinta Mountain lake cores, Utah, USA. Individual time series are shaded relative to their mean value. The histogram in the upper right presents the distribution of all LOI measurements. Core names are keyed to Table 1, and letter abbreviations correspond to Figure 1.

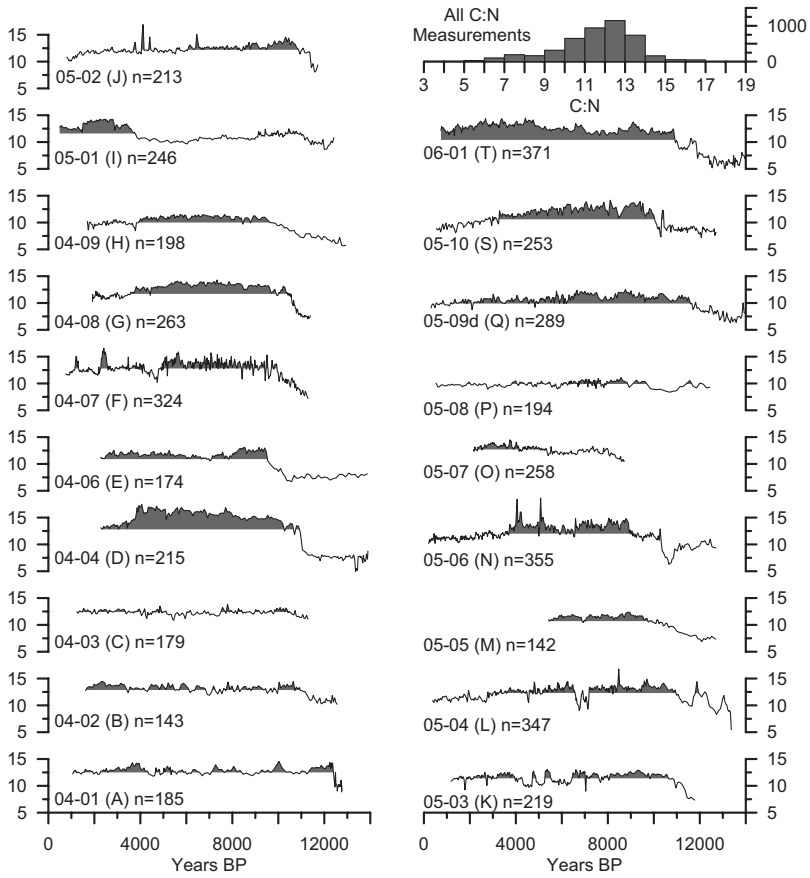

Figure 6. Time series of carbon-nitrogen ratio (C:N) measured in Uinta Mountain lake cores, Utah, USA. Individual time series are shaded relative to their mean value. The histogram in the upper right presents the distribution of all C:N measurements. Core names are keyed to Table 1, and letter abbreviations correspond to Figure 1.

2019). Measurement of the carbon-nitrogen ratio is less commonly employed because it requires an elemental analyzer. However, the effort and expense involved in making these measurements is worth it because unlike LOI, C:N is able to distinguish between terrestrial and aquatic organic matter sources (Meyers and Ishiwatari, 1993, 1995). Together these two proxies are useful for interpreting changes in lake productivity over time, as well as variations in the composition and amount of surrounding vegetation.

The grain size distribution of clastic material in lacustrine sediment reflects the energy of the sedimentary environment and the relative importance of various mechanisms in delivering clastic material to the coring site (e.g., Noren et al., 2002; Parris et al., 2010). These could include fluvial systems connected with the lake, colluvial processes operating on the surrounding slopes, sediment redistribution by currents within the lake, and eolian transport of dust to the lake surface. Shifts in grain size distribution over time, can be interpreted in terms of water level fluctuations, geomorphic stability in the surrounding watershed, the frequency of storms capable of delivering coarser material to locations far from shore, and other environmental changes (e.g., Brown et al., 2000; Xiao et al., 2009; Yellen et al., 2014; Liu et al., 2016).

To maximize their interpretive power, proxies measured in lake sediments are sometimes calibrated to modern conditions (e.g., Marshall et al., 2002). This was not possible in this study, however, because the uppermost sediment in most cores was not retrieved by the percussion coring equipment. Instead, two strategies are employed to overcome this potential limitation. First, values of individual proxy measurements are rarely considered in isolation. Rather, significance is assigned to along-core variations in proxies. In this manner, patterns of change over time, as opposed to numerical values, are the focus of interpretation. Second, whenever possible proxies are considered collectively in a multiproxy approach (e.g., Moreno et al., 2012; Johnson et al., 2013). This strategy reduces the ambiguity inherent in some of these measurements and permits more detailed interpretations.

Application of this approach to the Uinta lake data set revealed four consistent aspects of the post-glacial history of this environment. First, abundant submicron material in the deep parts of all cores attests to widespread landscape instability in the millennia after deglaciation. Second, rapidly rising values of LOI in deep sections of many cores represent the establishment of biologically productive conditions in the lake and surrounding watershed. Radiocarbon-based constraints support comparison of the onset of rising LOI values between different lakes. Third, grain size distributions in concert with changing values of LOI and C:N reveal a mid-Holocene interval during which greater volumes of terrestrial sediment were delivered to these lakes. Finally, lakes at the western end of the Uinta record a notable environmental perturbation ca. 4.5 ka BP. In the sections that follow, the evidence supporting each of these interpretations is presented and discussed.

Submicron Material

The abundance of submicron (colloidal) material in sediment cores from the Uinta Mountain lakes (Fig. 8) was unexpected because such fine material is not commonly reported from particle size distributions of lake sediments. Therefore, three tests were undertaken to confirm the presence of this material. First, a NIST 1 µm microbead standard was analyzed to verify the accuracy of the LA-950 analyzer. As expected, the analyzer detected this standard as a single, sharp peak focused at 1 µm. Second, because the particle size distributions resulting from laser scattering analysis are dependent on the refractive index of the minerals and the imaginary component used in calculations, these parameters were adjusted within reasonable bounds and a representative subset of samples was recalculated. In all cases, the prominent submicron peak was retained in the recalculated particle size distributions, indicating that this peak is not an artifact of the input parameters for the calculations. Finally, five samples assessed by the LA-950 as rich in submicron material were dispersed, vacuum filtered to <1 µm, and sent to Horiba in Irvine, California, USA, where they were analyzed with a LB-550 nano-particle analyzer. Analysis of all five samples revealed a sharp peak of submicron material, confirming the particle size distribution reported by the LA-950 (Fig. 9). Thus, it is concluded that submicron material is actually present in these sediment cores.

When considered relative to the depth-age models, the abundance of submicron material is

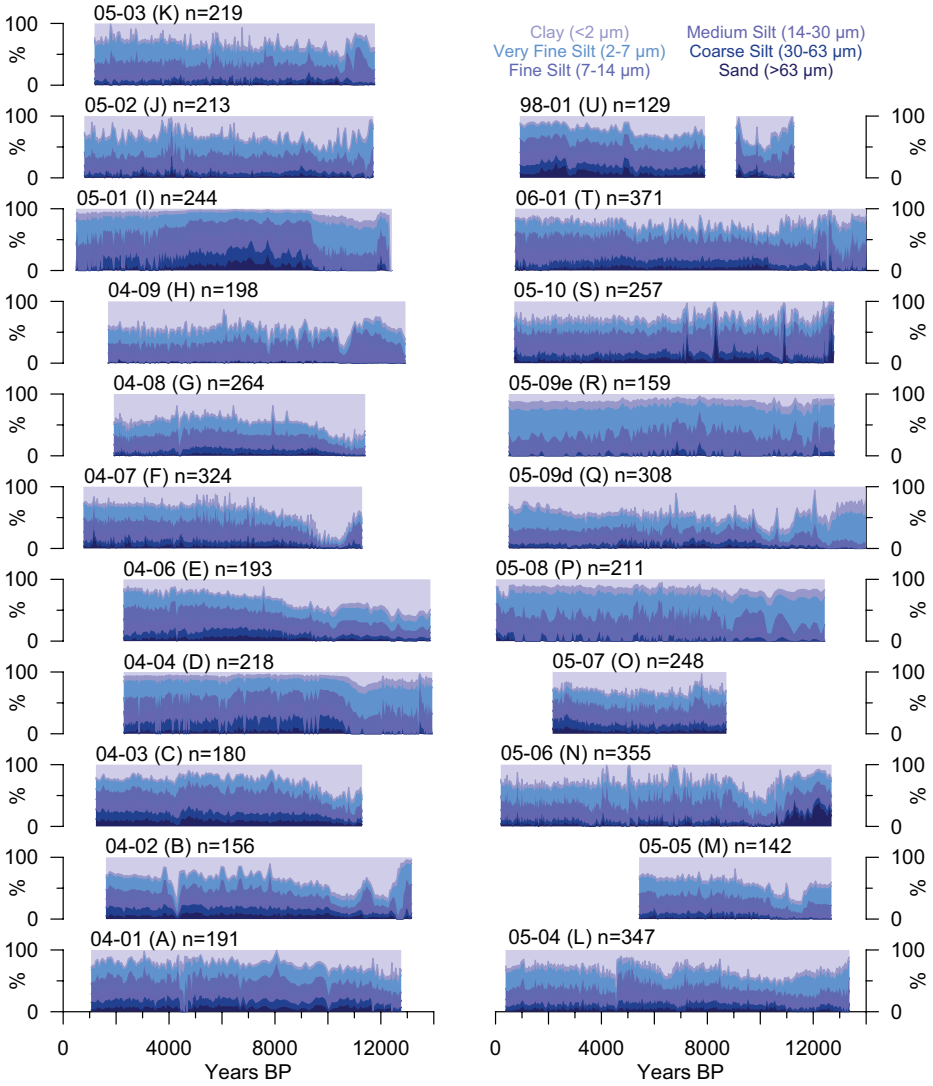

Figure 7. Time series of grain size distribution in Uinta Mountain lake cores, Utah, USA. Colored shading represents the abundance of grain size fractions from clay to sand, as shown in the key at upper right. Core names are keyed to Table 1, and letter abbreviations correspond to Figure 1.

notably higher in sediment that accumulated before ca. 9.5 ka BP (Fig. 8). To evaluate this pattern further, all of the submicron records were interpolated to a standard 50-year time step and recalculated as a Z-score (standard deviations away from the mean value in each core). Plotting the average Z-score for all of the records clarifies the consistency of this pattern (Fig. 8): between 12.0 and 9.5 ka BP the average Z-score for all records was consistently >0, with a maximum of 1.5 at ca. 10.3 ka BP. Even in cores where submicron material remained abundant later in the Holocene (for instance 05-02, 05-03, and 06-01), maximum values of submicron material abundance were recorded before 9.5 ka BP (Fig. 8).

The pattern of elevated submicron abundance has a strong spatial component as well. The highest values are associated with the lakes in the central part of the Uinta Mountains, whereas the lowest values are found in lakes from the eastern Uintas. Lakes at the far western end of the range have intermediate values of submicron material abundance. This pattern suggests that the abundance of submicron material is controlled by the location of each lake.

One possibility is that the submicron material reflects eolian processes, and that prevailing wind patterns deliver more of this material to lakes in the central and western Uintas. However, submicron material is not present in modern dust arriving at high elevations in the Uintas (Munroe, 2014; Munroe et al., 2015). The degree to which early Holocene dust may have differed from modern dust is unknown, yet it seems unlikely that submicron material could have been abundant in older dust when it is entirely absent today. Moreover, the physical and chemical properties of modern dust in the Uintas are remarkably consistent from one end of the range to the other (Munroe, 2014; Munroe et al., 2015), which does not support the idea that eolian submicron material was preferentially deposited in the central and western Uintas in the early Holocene.

A more likely possibility is that submicron material was derived from soils, regolith, and bedrock within the watersheds of the sampled lakes. Mineralogical analysis using X-ray diffraction reveals that the submicron material is primarily illite (Ebel and Munroe, 2015), which is common in Uinta soils (Douglass, 2000; Munroe, 2014) and is present in the shale layers interbedded with coarser clastic units in the Uinta Mountain bedrock (Myer, 2008). In this scenario, the submicron material in the lake cores was transported by fluvial and colluvial processes from the surrounding watershed. Additional support for this interpretation is provided by geochemical analysis of the fine (<20 μm) fraction of representative Uinta Mountain soils and samples of submicron material isolated from the early Holocene sections of cores 04-07, 04-08, 04-09, 05-01, 05-05, 05-06, and 05-10 (Ebel and Munroe, 2015). With the exception of 05-05, the submicron samples exhibit normalized rare earth element (REE) patterns that closely parallel those of the soil fine fraction (Fig. DR25; see footnote 1). Together the presence of illite in both the watershed materials and submicron samples, and their strongly similar REE abundance patterns, supports the interpretation that the submicron material in the lake cores was derived from the surrounding watersheds (Ebel and Munroe, 2015).

If the submicron material is locally sourced and transported to each lake by erosion, then the abundance of submicron material in each core can be considered a proxy for erosion in the surrounding watershed. The high abundances of submicron material in each lake before ca. 9.5 ka BP (Fig. 8), therefore, indicate that soils and regolith in these watersheds were unstable prior to that time. Given that all of these lakes are located in high elevation landscapes that became ice-free ca. 14.0 ka BP (Munroe and Laabs, 2017), this sustained instability likely reflects persistence of exposed loose sediment, sparse vegetation, and minimal soil development. Loss-on-ignition records indicate that organic matter accumulation in most lakes began ca. 11.0 ka BP (next section), but C:N val-

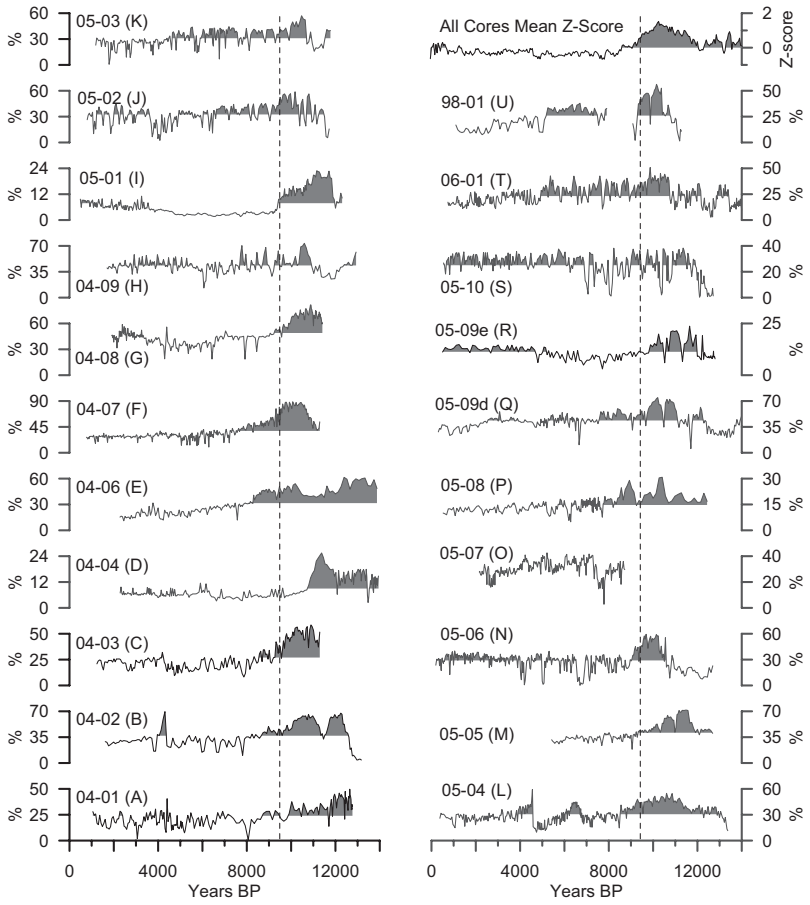

Figure 8. Plot of the abundance of submicron material in Uinta lake cores, Utah, USA. All curves are filled relative to their mean value. Core names are keyed to Table 1, and letter abbreviations correspond to Figure 1. The average Z-score for submicron abundance in all cores is shown in the upper right. Submicron material was notably more abundant in the early Holocene, and diminished greatly in abundance in most cores after 9.5 ka BP (vertical dashed line).

ues were initially low, indicating that this productivity was initially aquatic. An offset in the timing of aquatic versus terrestrial productivity may reflect the generally nutrient-poor nature of the quartz-dominated bedrock in the Uintas. Time may also have been required for eolian processes to deliver sufficient minerals bearing base cations and other necessary nutrients to the soils in these high elevation watersheds (Munroe, 2014; Munroe et al., 2015; Aciego et al., 2017; Arvin et al., 2017).

Timing and Nature of the Initial LOI Rise

All lake cores from the Uinta Mountains (except 04-03 and 05-07) penetrated to inorganic sediments that accumulated before the onset of biologic productivity in the lake and surrounding watershed. It is interesting, therefore, to compare the style of the initial LOI rise in these records between lakes. In most lakes this increase was gradual, occurring over several millennia (Fig. 5), however in five lakes (04-02, 05-01, 05-06, 06-01, and 98-01) this rise was notably abrupt (Figs. 5 and 10). In core 04-02, values of LOI increased from ~2% to ~8% in ~500 years, whereas in core 05-01, an increase from 2% to 10% occurred in ~300 years. In both of these cores, the increase occurred at ca. 12.3 ka BP. In the other three lakes, the LOI rise happened later, ca. 10.7 ka BP. The increase in 05-06 was from 2%–10%, in 98-01 from 10%–20%, and in 06-01 from 15%–35%. In four cores (excepting 98-01), this rise is tightly constrained by a radiocarbon date, supporting the interpretation that these stepwise LOI increases happened asynchronously in different groups of lakes. For comparison, in Colorado at Cumbres Bog, ~500 km southeast of the Uintas, and at Bison Lake and Upper Big Creek Lake ~250 km east of the Uintas, organic matter accumulation began ca. 11.5 ka BP (Johnson et al., 2013; Anderson et al., 2015; Shuman et al., 2015). Similar timing was reported for the end of glacially influenced sedimentation and the onset of rising LOI values at Jenny Lake in the Teton Mountains of Wyoming, USA (Larsen et al., 2016).

To determine whether the lakes (n = 5) in which LOI rose rapidly differ in a consistent manner from the lakes (n = 15) in which LOI rose gradually, variables describing lake morphology and physical setting generated by a separate study of watershed controls on lacustrine LOI values (Munroe, 2019) were compared between the two groups using a Mann-Whitney test (Fig. 11). Results reveal that the lakes where LOI rose rapidly are shallower ($P = 0.053$) than the other lakes and have both lesser surface areas ($P = 0.012$) and shorter perimeters ($P = 0.033$). These lakes are also surrounded by watersheds that are less rugged, with smaller maximum slopes ($P = 0.008$), mean slopes ($P = 0.053$), and slope ranges ($P = 0.008$), and less exposed bedrock ($P = 0.004$). In contrast, there is no significant difference in the elevation of the lakes in these two groups ($P = 0.672$), in the size of their watersheds ($P = 0.119$), in their watershed/lake area ratio ($P = 0.933$), or an obvious pattern in terms of where in the Uintas they are located.

The two lakes (04-02 and 05-01) in which the LOI rise occurred earlier (ca. 12.3 ka BP) are larger than the lakes in which the rise happened ca. 10.7 ka BP. These "early" lakes also have greater lake area/depth ratios, longer perimeters, generally lower elevation watersheds, and a greater number of inflowing streams. These differences are not significant because of the small number of lakes in the two groups. However, they nonetheless suggest that lakes in the "early" group may have had warmer water temperatures in the latest Pleistocene; that these lakes might have had more extensive, productive littoral zones; and that more terrestrial organic matter was delivered to them by inflowing streams.

Overall, this analysis reveals that smaller, shallower lakes in gently sloping watersheds with extensive areas mantled by soil where vegetation could become established experienced rapid increases in LOI rise at the Pleistocene/Holocene transition. In contrast, larger, deeper lakes in rugged watersheds containing large areas of exposed rock (with correspondingly reduced vegetation cover) took longer to reach peak levels of aquatic and terrestrial productivity. Although focused solely on LOI, this result provides a cautionary note for paleolimnological studies, emphasizing the degree to which lakes may record paleoclimate changes, such as the warming into the Holocene, differently depending on their dimensions and physical setting (Munroe, 2007a, 2019; Corbett and Munroe, 2010).

TABLE 3. ABUNDANCES OF CLAY AND SUBMICRON MATERIAL IN UINTA MOUNTAIN LAKE CORES, UTAH, USA

Fig. 1 code	Lake ID	Lake name	Max 2–1 μm (%)	Year BP	Mean 2–1 μm 12–10 ka BP (%)	Max <1 μm (%)	Year BP	Mean <1 μm 12–10 ka BP (%)	Ratio
A	04-01	Marshall	13.6	12416	4.1	49.7	12648	31.4	7.7
B	04-02	Hoover	12.7	12660	5.1	65.9	12295	55.2	10.8
C	04-03	Pyramid	6.2	11007	4.1	58.5	10895	50.1	12.2
D	04-04	Elbow	14.9	13418	8.7	25.5	11378	14.8	1.7
E	04-06	Swasey	14.3	14554	6.3	61.4	12389	43.7	6.9
F	04-07	Spider	7.5	11254	4.6	88.2	9770	68.5	14.9
G	04-08	Little Superior	6.6	11203	3.7	81.4	10895	70.9	19.2
H	04-09	North Star	8.0	12932	4.1	73.6	10598	43.5	10.6
I	05-01	Reader	12.8	10094	10.4	29.9	11157	16.1	1.5
J	05-02	Ostler	7.1	11438	3.9	58.8	10178	34.2	8.8
K	05-03	Kermsuh	11.5	10959	5.6	57.0	10474	36.1	6.4
L	05-04	Ryder	8.5	12149	4.7	54.9	10609	44.3	9.4
M	05-05	Lower Red Castle	6.4	11743	4.7	71.1	11485	57.1	12.1
N	05-06	Bald	9.7	11323	5.8	59.4	9683	29.9	5.2
O	05-07	Hessie	4.0	7244	--	42.6	5211	--	--
P	05-08	Deadhorse	14.8	12292	11.1	30.8	10214	20.5	1.8
Q	05-09d	Island	21.9	13979	6.4	74.6	10358	56.2	8.8
Q	05-09e	Island	14.1	12227	11.5	23.7	11647	16.3	1.4
R	05-10	Taylor	16.9	10742	5.7	38.4	11885	26.8	4.7
S	06-01	Upper Lily Pad	20.4	12564	3.9	50.8	9870	28.0	7.2
T	98-01	Hacking	8.1	10759	5.1	56.2	10153	30.2	5.9
--	--	Overall mean	11.4	11760	6.0	54.9	10657	38.7	7.9

Early Holocene Storminess

Loss on ignition is a useful proxy for the organic matter content of lake sediments (Dean, 1974), however it cannot uniquely discriminate between organic matter of terrestrial and aquatic provenance. In contrast, C:N is sensitive to the source of the organic matter, with terrestrial material having greater C:N values (Meyers and Ishiwatari, 1993, 1995). These two proxies can be considered together, therefore, to reveal whether higher organic matter contents reflect increased in-lake productivity or enhanced influx of terrestrial material. Inverting this logic, in a lake where organic matter abundance is strongly controlled by the input of terrestrial organic material, a positive correlation between LOI and C:N should exist. Conversely, in a lake where aquatic productivity is dominant, this correlation should be negative.

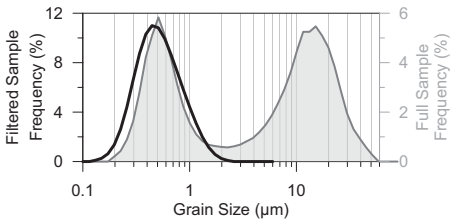

Figure 9. Example grain size distribution plot illustrating the presence of abundant submicron (<1 μm diameter) particles in Uinta lake sediment, Utah, USA. The sample is from a depth of 180–182 cm in core 05-08, corresponding to an age of ca. 10 ka BP. The gray distribution in the background represents the complete sample, whereas the black line in the foreground represents the grain size distribution after vacuum filtering to 1 μm and analysis with a nanoparticle analyzer.

The relationship between LOI and C:N in the Uinta lake cores was assessed with Spearman's rank correlation (Table DR3; see footnote 1). This nonparametric test was utilized because nearly all of the LOI and C:N data sets for individual lakes are non-normally distributed ($P<0.05$ with a Shapiro-Wilk test). Values of Spearman's rho (ρ) range from a maximum of 0.922 (core 04-08) to a minimum of –0.293 (core 05-08). Values in eight lakes are >0.6, and P-values are <0.04 in all but two lakes (04-01 and 05-02). Notably, a consistent relationship exists between ρ values and hydrologic setting characterized in previous work (Munroe, 2007a; 2019), with higher ρ values corresponding to lakes with (a) a greater number of inflows, (b) larger volume inflows, (c) perennial inflows, and (d) steeply sloping watersheds. Conversely, many of the lakes with low ρ values are characterized by a lack of robust, inflowing streams (Table DR3). This relationship is consistent with a model in which the amount of terrestrial organic matter delivered to a lake from the surrounding watershed controls the organic content of the lacustrine sediment.

This relationship is further developed through consideration of the grain size distribution measured by particle size analysis. Because these cores were collected from deep water far from major inlets, particularly high-volume inflows would be necessary to transport coarser material to the coring site. On the basis of modern observations, such inflows are typically associated with intense rainstorms. Given the average time resolution of the 1 cm samples analyzed for grain size distribution, and the bioturbated nature of some of the sediments, it is not possible to resolve individual storm events in these cores—with the possible exception of the prominent graded beds in cores 05-09e and 05-10. Instead, coarser sediment overall, and the presence of sand grains (>63 um) in particular, are considered a signal of "storminess" (e.g., Noren et al., 2002; Parris et al., 2010), highlighting time intervals in which high-intensity storms

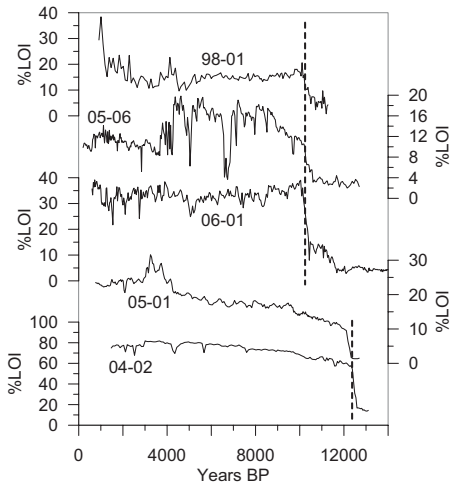

Figure 10. Time series of loss-on-ignition (LOI) in the five lake sediment cores exhibiting an abrupt rise in organic matter content (as revealed by %LOI) in the latest Pleistocene/early Holocene. The LOI increase occurred earlier in cores 04-02 and 05-01 (ca. 12.3 ka BP), and later in cores 06-01, 05-06, and 98-01 (ca. 10.7 ka BP). The age of this increase is interpolated in core 98-01, but is tightly constrained by radiocarbon dates in the others.

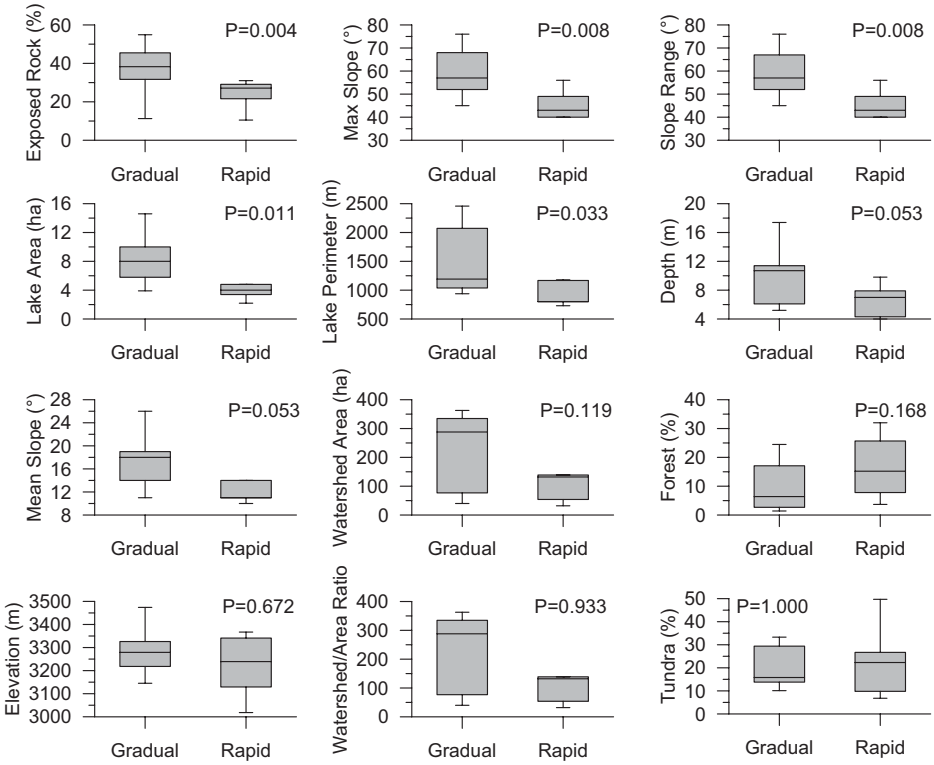

Figure 11. Box plots presenting the differences in various watershed and lake properties between lakes exhibiting a gradual loss-on-ignition LOI rise, and those exhibiting a rapid rise in the Uinta Mountains, Utah, USA (Fig. 10). Plots are arranged from the most significant difference (upper left), to least significant difference (lower right).

were common enough to change the grain size distribution of sediment accumulating far out in the center of the lake basin.

The combination of LOI, C:N, median grain size, and sand content provides, therefore, a framework for identifying intervals of enhanced storminess. The greater hydrologic inflow associated with storms would wash more terrestrial organic matter and clastic material farther out into the lake, increasing LOI, C:N, median grain size, and the abundance of sand grains. Given this model, the values for these four proxies in the six lakes (04-08, 04-04, 04-09, 05-05, 05-09d, and 05-04) with major surface inflows and the strongest correlation between LOI and C:N (Table DR3) were converted to Z-scores and averaged. To focus on relatively organic-rich sediments, only the Holocene section of each core (<11.7 ka BP) was considered. Results reveal that Z-score sums were consistently high in the early part of the Holocene, particularly between ca. 10 and 6 ka BP (Fig. 12). The lakes exhibiting this pattern are found throughout the Uintas, and are not focused on one end or one side of the range (Fig. 1). Enhanced precipitation leading to greater inflows, therefore, appears to have been characteristic of climate throughout the Uinta Mountains in the early Holocene.

Some previous work has interpreted changes in the organic content and grain size distribution of lacustrine sediments as a signal of fluctuating water level, which moves the littoral zone (where sediments are characteristically coarser and less organic-rich) closer to or farther from the lake center (e.g., Shuman et al., 2009, 2015; Shuman and Serravezza, 2017). However, this model cannot explain the proxy patterns in these deepwater cores from the Uintas, where organic content and sediment coarseness rise in concert (along with an increase in the abundance of terrestrial organic matter measured by C:N).

Convective thunderstorms with high-intensity precipitation that may lead to brief increases in the influx of terrestrial material are particularly common in the Uintas during summer months when the North American Monsoon (NAM) delivers moisture from the south. The NAM forms over northwestern Mexico in mid-summer and impacts areas farther north to a diminishing degree between July and September (Ropelewski et al., 2005). The Uintas are located at the northern boundary of the region reached by the NAM (Mock, 1996; Metcalfe et al., 2015). However, most precipitation records there demonstrate an increase in August precipitation over July, consistent with increased convective storm activity driven by moisture delivery in late summer (fig. 5 in Mock, 1996).

Considerable research has focused on reconstructing the history of the NAM during the post-glacial period (e.g., Adams and Comrie, 1997). Monsoonal dynamics are driven by unequal heating of land and ocean surfaces, and modeling studies have concluded that the NAM was stronger in the early Holocene in response to enhanced summer insolation (Diffenbaugh et al., 2006; Zhao and Harrison, 2012). At the same time, changes in atmospheric circulation induced by the lingering Laurentide Ice Sheet appear to have delayed the peak of NAM activity in the southwestern U.S. relative to the summer insolation (Metcalfe et al., 2015). In paleoclimate records from the southwestern U.S., the NAM was well established by 9 ka BP, and reached a peak geographic extent ca. 6 ka BP (Metcalfe et al., 2015). This temporal pattern corresponds clearly with the ca. 10–6 ka BP interval of enhanced terrestrial influx to Uinta lakes, supporting the interpretation that a strengthened early Holocene monsoon resulted in more frequent high intensity precipitation events in the Uintas (Fig. 12).

Furthermore, it is notable that this interval of enhanced influx of terrestrial material (ca. 10–6 ka BP) straddles an early Holocene humid period (11–8 ka BP) and the onset of mid-Holocene aridity (8–5.5 ka BP) in the Rocky Mountains seen in an extensive compilation of lake level records (Shuman and Serravezza, 2017). Thus, lakes with prominent inflowing streams in the Uinta Mountains were subject to more frequent and/or larger magnitude terrestrial influx events during times when regional hydroclimate was both wetter and drier (Fig. 12). This overlap might at first appear contradictory, but intense precipitation events are possible under conditions of both increased and decreased annual precipitation. Thus, this overlap is additional support for the interpretation that LOI, C:N, and sediment coarseness in deepwater cores from Uinta lakes record the frequency of influx, not lake level changes.

Finally, it is also possible that high volume inflows in the early Holocene were driven not by summer storms, but rather by rapid melting of deeper winter snowpack in the spring. For instance, a winter-sensitive speleothem from a cave ~175 km northwest of the Uintas records notably wet (and/or colder) conditions from 9.5 to 7.4 ka BP (Lundeen et al., 2013), overlapping the ca. 10–6 ka BP interval of enhanced influx of terrestrial material seen in the Uinta lakes (Fig. 12). Similarly, Bear Lake, located in a winter-dominated precipitation regime (Dean et al., 2009) near this cave, contains sedimentary evidence for transgressions to higher water

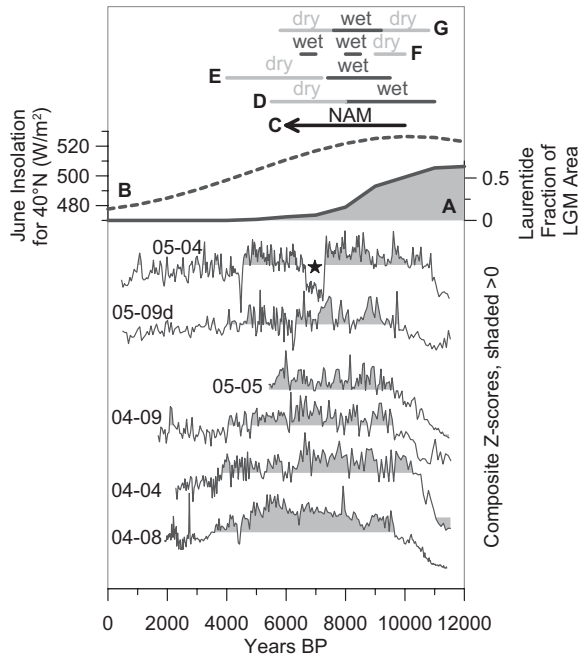

Figure 12. Z-score sums for loss-on-ignition (LOI), carbon-nitrogen ratio (C:N), median grain size, and % sand (>63 μm) in the six studied lakes in the Uinta Mountains, Utah, USA exhibiting robust inflows and the strongest correlation between LOI and C:N. All records are consistently above 0 (shaded) throughout the interval ca. 10–6 ka BP, suggesting more frequent influx of terrestrial material consistent with high intensity precipitation events. The abrupt departure in core 05-04 (star) is interpreted to reflect a temporary change in the configuration of inflowing streams. Other paleoclimate records are shown for reference: (A) Remaining fraction of the Laurentide Ice Sheet relative to full Last Glacial Maximum (LGM) extent (Shuman et al., 2005). (B) June insolation for 40°N (Berger and Loutre, 1991). (C) Increasing strength of the North American Monsoon (NAM) in the southwestern U.S. (Metcalfe et al., 2015). (D) Intervals of wetter and drier hydroclimate in the Rocky Mountain region inferred from lake level reconstructions (Shuman and Serravezza, 2017). (E) Intervals of drier and wetter climate in northern Utah inferred from a winter-sensitive speleothem (Lundeen et al., 2013). (F) Intervals of wetter and drier conditions at Bear Lake, Utah inferred from sedimentary evidence (Smoot and Rosenbaum, 2009). (G) Intervals of wetter and drier conditions at Bear Lake, Utah inferred from diatoms (Moser and Kimball, 2009).

levels between 8.5 and 8.0 and 7.0–6.5 ka BP (Smoot and Rosenbaum, 2009) and diatom evidence for higher water from 9.2 until 7.6 ka BP (Moser and Kimball, 2009). Unfortunately, no stream gage data exist for high-elevations in the Uintas. As a result it is unclear whether flows produced by the relatively slow process of snowmelt are an important mechanism for delivering terrestrial material to lakes in these small, gently sloping, well-vegetated watersheds. In contrast, first-hand observations have repeatedly confirmed that intense rainstorms associated with summer thunderstorms mobilize and transport large amounts of both organic and inorganic terrestrial sediments to these lakes. Overall, the summer storminess interpretation is preferred here, but future work should be targeted at evaluating the possible role of snowmelt.

Evidence for a Climatic Perturbation ca. 4.5 ka BP

Multiproxy records from all six lakes at the western end of the Uintas (04-01, 04-02, 04-03, 05-02, 05-03, and 05-04, Fig. 1) exhibit a notable shift ca. 4.5 ka BP, where values of LOI and C:N dropped at the same time that the sediment became notably finer. Radiocarbon dates closely constrain the age of this event in four of the lakes (04-01, 04-02, 04-03, and 05-04); all of these ages have calibration ranges that overlap ca. 4.5 ka BP (Fig. 13). To highlight the uniqueness of this event, values of LOI, C:N, and median grain size were converted to Z-scores and averaged to yield an event index for each record. Plotting this index on a common time scale reveals that Z-scores in all lakes dropped to as low as 2.3 standard deviations below the mean at this time (Fig. 13). Furthermore, in lakes 04-02, 04-03, 05-03, and 05-04, where the abundance of biogenic silica (bSi) was quantified across this interval, bSi fell synchronously with Z-score (Fig. 13).

In all cores, the interval of decreased Z-scores spans several cm, suggesting an event duration of a few centuries. Furthermore, in four of the cores (04-01, 04-02, 04-03, and 05-04) this event interval contains a thin (~1-cm-thick), light gray (10YR 5/1) clay layer that contrasts strongly with the darker, more organic-rich sediment above and below. A concentration of conifer needles was present immediately below this layer in 04-02, and in 04-01 the clay contained a piece of wood along with a small (~1-cm-diameter) pebble.

This event must have been caused by an environmental change spanning the western Uintas, rather than an isolated event specific to just a single watershed. One possibility is that it simply represents an unusually strong rainstorm that washed large amounts of terrestrial material into these lakes. As the surrounding bedrock is predominantly light gray to white in this part of the Uintas, this would explain the color of the layer, and a pulse of clastic material would dilute the organic matter in the sediment, reducing LOI and bSi. On the other hand, a rainstorm strong enough to flood these lakes with terrestrial material would likely have increased the average grain size at the coring site, as discussed above. Yet a hallmark of this event is a dramatic decrease in grain size; in 04-02, for example, the median grain size of the clay layer is just ~0.2 μm. Furthermore, the clay layer, which could conceivably represent settling of clastic material at a point in the lake remote enough to not be affected by influx of coarser material, is just a part of multi-cm-thick interval in which LOI, C:N, and median grain size were all depressed.

Another possibility is that this event represents a time in which winter snowpack was notably deeper and these lakes and watersheds remained ice and snow-covered for most or all of the summer. Given their upwind position, the western Uintas receive more snow than the rest of the range today (MacDonald and Tingstad, 2007), and even under the modern climate, some lakes remain frozen and snow-covered through June. An enhancement of the snowpack would lengthen the duration of this snow-covered period each year, depressing organic productivity (as represented by LOI and C:N) and reducing the amount of coarser clastic material entering the lakes (decreasing the median grain size). In this scenario, the clay layer may have accumulated during a time when the lakes remained snow-covered for multiple consecutive years, allowing fine material to settle in calm water beneath the ice. The pebble in 04-01, and the concentration of conifer needles in 04-02, may have been delivered to the coring site by avalanching onto the lake ice. Lakes farther east in the Uintas, where winter snowpack is typically thinner, may not have experienced such a dramatic shift in the average duration of annual ice cover.

Although the nature and cause of the event seen in the western Uinta sediment cores ca. 4.5 ka BP remain unclear, other studies have reported paleoclimatic shifts at approximately the same time. For instance, numerous records document a severe drought in the midconti-

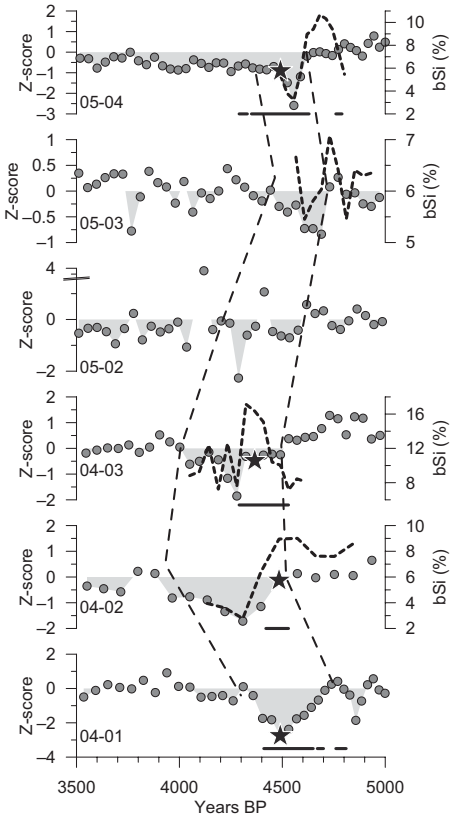

Figure 13. All six lake (Fig. 1) cores from the western Uintas, Utah, USA, contain evidence for a climatic perturbation at ca. 4.5 ka BP. The signature of this event is a transient, but notable, decrease in loss-on-ignition, carbon-nitrogen ratio, and median grain size. Here, values for those proxies are converted to Z-scores and summed for each lake to highlight this interval. Dots mark individual data points and the gray shading highlights depression below the mean value. In four lakes, the abundance of biogenic silica (bSi) was also measured. These values are plotted as dotted, black lines illustrating that bSi decreased synchronously with the changes in the other proxies. Stars in 04-01, 04-02, 04-03, and 05-04 mark the locations of radiocarbon dates. The gray bars beneath the stars designate the 2-σ calibration ranges for these ages, emphasizing their overlap. Dashed vertical lines highlight the correspondence, within the dating uncertainty, of the event in the six records.

nent of the U.S. and in the Rocky Mountains ca. 4.2 ka BP (Booth et al., 2005; Carter et al., 2018), and a diatom record from the northern Rocky Mountains indicates a change in dominant hydroclimate at ca. 4.5 ka BP (Stone and Fritz, 2006). Records from the Great Basin west of the Uintas are consistent with wetter conditions between ca. 5 and 3.7 ka BP (as reviewed in Noble et al., 2016). Composites of globally distributed paleoclimate records also reveal an interval of rapid climate change 4.2–3.8 ka BP (Mayewski et al., 2004), following a notably cold event ca. 4.7 ka BP (Wanner et al., 2011). Thus, it is possible that lakes in the western Uintas responded to these same climatic perturbations.

Limitations and Directions for Future Work

Collective consideration of the large number of cores retrieved and analyzed in this study mitigated some of the uncertainties inherent in interpretation of LOI, C:N, and grain size records. However, some ambiguities remain that could be addressed by future work. For instance, biogenic silica could be analyzed throughout the complete set of cores to provide another perspective on lacustrine productivity that would be useful in interpreting the timing of the initial LOI rise (e.g., Conley and Schelske, 2002). Geochemical analysis of the clastic fraction of these sediments could reveal weathering trends related to the establishment of soil cover in the surrounding watersheds during the immediate post-glacial period (e.g., Mourier et al., 2010). Study of pollen could elucidate whether the enhanced delivery of terrestrial material in the early Holocene occurred primarily during the spring or summer seasons (e.g., Gauthier and Muñoz, 2009). That distinction would clarify whether rapid spring snowmelt or more energetic summer thunderstorms were responsible for the increased erosion of material from the watershed. Finally, additional radiocarbon dating and perhaps identification of cryptotephras would further refine the age models (e.g., Davies, 2015). This improvement would facilitate further comparison of the records, and would help evaluate the synchronicity of the 4.5 ka BP event in the western Uinta lake cores.

CONCLUSION

Sedimentary cores spanning the post-glacial period were collected from 20 lakes in the Uinta Mountains of northeastern Utah. Development of depth-age models for these cores through ^{14}C dating, combined with multiproxy analysis (loss-on-ignition, carbon-nitrogen ratio, and grain size distribution), revealed several notable aspects of post-glacial climatic history in this mountain range. Significantly, the large number of cores examined in this study (Fig. 14) permitted the identification of paleoenvironmental variability that might have been overlooked or misinterpreted in a focused study of a smaller data set.

Lakes throughout the Uintas accumulated strikingly high abundances of submicron material, primarily illitic clay, during the latest Pleistocene and early Holocene (Figs. 8 and 14). Notably, accumulation of this material diminished greatly in nearly all lakes at 9.5 ka BP. The presence of illite with similar rare earth element abundance patterns in shaley facies of the Uinta Mountain bedrock and in soils suggests that this material was eroded from the watersheds surrounding these lakes by fluvial and colluvial processes. This submicron material is interpreted, therefore, an indication of sustained landscape instability at higher elevations in the Uintas in the millennia following deglaciation.

Nearly all of the sediment cores considered in this study penetrated to inorganic silty clay recording sedimentation before the onset of biologic productivity in the lake and surrounding watershed. In many lakes, the rise in organic matter content was gradual through the early Holocene, signaling steadily increasingly established vegetation and aquatic productivity (Fig. 5). However, in five lakes the onset of organic sedimentation was very abrupt, occurring in just a few centuries (Fig. 10). These lakes are smaller and shallower than lakes exhibiting a gradual LOI rise, and are surrounded by less rugged watersheds with less exposed bedrock (Fig. 11). This contrast suggests that smaller, shallower lakes in gently sloping watersheds were rapidly colonized by both terrestrial and aquatic flora and fauna. In contrast, this process required several millennia in larger, deeper lakes in rugged watersheds with abundant exposed rock.

The rapid LOI rise occurred notably earlier (ca. 12.3 ka BP) in two lakes and later (ca. 10.7 ka BP) in three lakes (Figs. 10 and 14). The lakes exhibiting the early LOI rise are larger and have greater lake area/depth ratios, longer perimeters, generally lower elevation watersheds, and a greater number of inflowing streams. These characteristics may have made these lakes warmer in the latest Pleistocene, whereas larger amounts of organic matter could have been produced in their extensive littoral zones and delivered by inflowing streams.

Values of loss-on-ignition (LOI) and carbon-nitrogen ratio (C:N) exhibit a significant positive correlation in nearly all lakes, and this

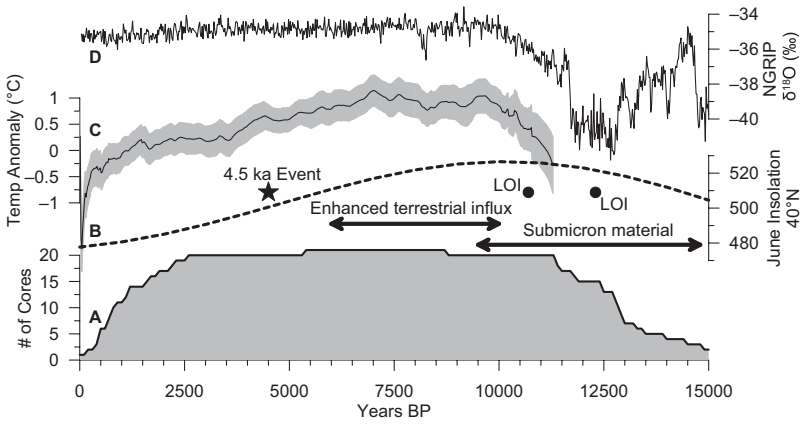

Figure 14. Summary of the Uinta Mountain lacustrine records, Utah, USA, compared with other paleoclimate data. Landscape instability leading to delivery of submicron material to lakes prevailed from ca. 15–9.5 ka BP. Enhanced influx of coarser clastic material and terrestrial organic matter, interpreted as a signal of storminess, extended from ca. 10–6 ka BP. Two lakes exhibited rapid increases in loss-on-ignition (LOI) at 12.3 ka BP, whereas three lakes record a similarly abrupt rise at 10.7 ka BP (dots). All lakes cored at the western end of the Uintas contain evidence for an environmental perturbation at 4.5 ka BP. (A) Number of cores in the Uinta lake data set. (B) June insolation for 40°N (Berger and Loutre, 1991). (C) Stacked temperature anomaly for 30–90°N with 1-σ error range (Marcott et al., 2013). (D) Stable isotope ($\delta^{18}O$) values for the North Greenland Ice Core Project (NGRIP) ice core on the Greenland Ice Core Chronology 2005 "GICC05" timescale (Rasmussen et al., 2006; Vinther et al., 2006).

correlation is particularly strong in lakes with major inflowing streams. This correspondence suggests that the abundance of organic matter in these lakes is controlled by the amount of terrestrial material delivered to lakes. Furthermore, sediment coarseness, and the abundance of sand grains specifically, increase in these lakes between 10 and 6 ka BP, simultaneous with higher values of LOI and C:N. This pattern is interpreted as a sign that lakes in the Uintas were subjected to increased influx of terrestrial material in the early Holocene (Figs. 12 and 14). Considering the modern climate of the Uintas, and other paleoclimatic data from the southwestern U.S., this enhanced influx is interpreted as a signal of increased storminess, likely driven by a strengthened North American Monsoon in the early to middle Holocene.

Finally, all lakes cored in the western Uintas record evidence of a paleoenvironmental perturbation around 4.5 ka BP (Figs. 13 and 14). The nature of this event is unclear, but its hallmarks include major decreases in LOI and C:N coupled with increases in the abundance of fine particles. In lakes where it was measured, the abundance of biogenic silica also decreases simultaneously. This pattern fits with other regional and global reports of rapid paleoenvironmental changes at approximately the same time.

ACKNOWLEDGMENTS

This project would not have been possible without the field assistance of M. Devito, D. Douglass, D. Munroe, S. Munroe, N. Oprandy, C. Plunkett, and C. Savage; along with Middlebury College students C. Anderson, D. Berkman, L. Corbett, and C. Rodgers; and Gustavus Adolphus College students T. Kohorst, K. Lawson, and A. Rishavy. Thanks to D. Koerner with the Ashley National Forest for arranging critical logistical support. Middlebury College students M. Bigl, L. Corbett, L. Duran, R. Ebel, G. Eglite, E. Ellenberger, S. Hamilton, and F. Hobbs contributed to the laboratory analyses. Funding was provided by NSF-EAR-0345112, NSF-ATM-0402328, and EAR-0922940 to J. Munroe. The Leco thermogravimetric analyzer was purchased with support from Vermont's Established Program to Stimulate Competitive Research. Thanks to Associate Editor John Jansen and two anonymous reviewers for comments and suggestions that improved the manuscript.

REFERENCES CITED

Abbott, M.B., Finney, B.P., Edwards, M.E., and Kelts, K.R., 2000, Lake-level reconstruction and paleohydrology of Birch Lake, central Alaska, based on seismic reflection profiles and core transects: Quaternary Research, v. 53, p. 154–166, https://doi.org/10.1006/qres.1999.2112.

Aciego, S.M., Riebe, C.S., Hart, S.C., Blakowski, M.A., Carey, C.J., Aarons, S.M., Dove, N.C., Botthoff, J.K., Sims, K.W.W., and Aronson, E.L., 2017, Dust outpaces bedrock in nutrient supply to montane forest ecosystems: Nature Communications, v. 8, no. 14800, https://doi.org/10.1038/ncomms14800.

Adams, D.K., and Comrie, A.C., 1997, The North American Monsoon: Bulletin of the American Meteorological Society, v. 78, p. 2197–2213, https://doi.org/10.1175/1520-0477(1997)078<2197:TNAM>2.0.CO;2.

Anderson, L., 2011, Holocene record of precipitation seasonality from lake calcite $\delta^{18}O$ in the central Rocky Mountains, United States: Geology, v. 39, p. 211–214, https://doi.org/10.1130/G31575.1.

Anderson, L., 2012, Rocky Mountain hydroclimate: Holocene variability and the role of insolation, ENSO, and the North American Monsoon: Global and Planetary Change, v. 92–93, p. 198–208, https://doi.org/10.1016/j.gloplacha.2012.05.012.

Anderson, L., Brunelle, A., and Thompson, R.S., 2015, A multi-proxy record of hydroclimate, vegetation, fire, and post-settlement impacts for a subalpine plateau, central Rocky Mountains, U.S.A: The Holocene, v. 25, p. 932–943, https://doi.org/10.1177/0959683615574583.

Arvin, L.J., Riebe, C.S., Aciego, S.M., and Blakowski, M.A., 2017, Global patterns of dust and bedrock nutrient supply to montane ecosystems: Science Advances, v. 3, no. 12, eaao1588.

Atwood, W.W., 1908, Lakes of the Uinta Mountains: Bulletin of the American Geographical Society, v. 40, p. 12–17, https://doi.org/10.2307/197991.

Atwood, W.W., 1909, Glaciation of the Uinta and Wasatch mountains: U.S. Government Printing Office, v. 61, https://doi.org/10.3133/pp61.

Berger, A., and Loutre, M.F., 1991, Insolation values for the climate of the last 10 million years: Quaternary Science Reviews, v. 10, p. 297–317, https://doi.org/10.1016/0277-3791(91)90033-Q.

Birks, H.H., and Birks, H.J.B., 2006, Multi-proxy studies in palaeolimnology: Vegetation History and Archaeobotany, v. 15, p. 235–251, https://doi.org/10.1007/s00334-006-0066-6.

Blaauw, M., 2010, Methods and code for 'classical' age-modelling of radiocarbon sequences: Quaternary Geochronology, v. 5, p. 512–518, https://doi.org/10.1016/j.quageo.2010.01.002.

Bockheim, J.G., and Munroe, J.S., 2014, Organic carbon pools and genesis of alpine soils with permafrost: A review: Arctic, Antarctic, and Alpine Research, v. 46, p. 987–1006, https://doi.org/10.1657/1938-4246-46.4.987.

Booth, R.K., Jackson, S.T., Forman, S.L., Kutzbach, J.E., Bettis Iii, E.A., Kreigs, J., and Wright, D.K., 2005, A severe centennial-scale drought in midcontinental North America 4200 years ago and apparent global linkages: The Holocene, v. 15, p. 321–328, https://doi.org/10.1191/0959683605hl825ft.

Bradley, W.H., 1936, Geomorphology of the north flank of the Uinta Mountains: U.S. Geological Survey Professional Paper 185-I, https://doi.org/10.3133/pp185I.

Brown, S.L., Bierman, P.R., Lini, A., and Southon, J., 2000, 10 000 yr record of extreme hydrologic events: Geology, v. 28, p. 335–338, https://doi.org/10.1130/0091-7613(2000)28<335:YROEHE>2.0.CO;2.

Brown, T.A., Nelson, D.E., Mathewes, R.W., Vogel, J.S., and Southon, J.R., 1989, Radiocarbon dating of pollen by accelerator mass spectrometry: Quaternary Research, v. 32, p. 205–212, https://doi.org/10.1016/0033-5894(89)90076-8.

Carter, V.A., Brunelle, A., Minckley, T.A., Dennison, P.E., and Power, M.J., 2013, Regionalization of fire regimes in the Central Rocky Mountains, USA: Quaternary Research, v. 80, p. 406–416, https://doi.org/10.1016/j.yqres.2013.07.009.

Carter, V.A., Shinker, J.J., and Preece, J., 2018, Drought and vegetation change in the central Rocky Mountains and western Great Plains: Potential climatic mechanisms associated with megadrought conditions at 4200 cal yr BP: Climate of the Past, v. 14, p. 1195–1212, https://doi.org/10.5194/cp-14-1195-2018.

Cohen, A.S., 2003, Palaeolimnology: The History and Evolution of Lake Systems: New York, USA, Oxford University Press, 500 p.

Conley, D.J., and Schelske, C.L., 2002, Biogenic silica, *in* Smol, J.P., Birks, H.J.B., Last, W.M., Bradley, R.S., and Alverson, K., eds., Tracking Environmental Change Using Lake Sediments: Dordrecht, The Netherlands, Springer, p. 281–293, https://doi.org/10.1007/0-306-47668-1_14.

Corbett, L.B., and Munroe, J.S., 2010, Investigating the influence of hydrogeomorphic setting on the response of lake sedimentation to climatic changes in the Uinta Mountains, Utah, USA: Journal of Paleolimnology, v. 44, p. 311–325, https://doi.org/10.1007/s10933-009-9405-9.

Dahms, D., Egli, M., Fabel, D., Harbor, J., Brandová, D., de Castro Portes, R., and Christl, M., 2018, Revised Quaternary glacial succession and post-LGM recession, southern Wind River Range, Wyoming, USA: Quaternary Science Reviews, v. 192, p. 167–184, https://doi.org/10.1016/j.quascirev.2018.05.020.

Davies, S.M., 2015, Cryptotephras: The revolution in correlation and precision dating: Journal of Quaternary Science, v. 30, p. 114–130, https://doi.org/10.1002/jqs.2766.

Davis, P.T., Menounos, B., and Osborn, G., 2009, Holocene and latest Pleistocene Alpine glacier fluctuations: A global perspective: Quaternary Science Reviews, v. 28, p. 2021–2033, https://doi.org/10.1016/j.quascirev.2009.05.020.

Dean, W.E., Jr., 1974, Determination of carbonate and organic matter in calcareous sediments and sedimentary rocks by loss on ignition: Comparison with other methods: Journal of Sedimentary Petrology, v. 44, p. 242–248, https://doi.org/10.1306/74D729D2-2B21-11D7-8648000102C1865D.

Dean, W.E., Wurtsbaugh, W.A., and Lamarra, V.A., 2009, Climatic and limnologic setting of Bear Lake, Utah and Idaho, *in* Rosenbaum, J.G., and Kaufman, D.S., eds., Paleoenvironments of Bear Lake, Utah and Idaho, and its catchment: Geological Society of America Special Paper 450, p. 1–14, https://doi.org/10.1130/2009.2450(01).

Dehler, C.M., Porter, S.M., De Grey, L.D., Sprinkel, D.A., and Brehm, A., 2007, The Neoproterozoic Uinta Mountain Group revisited: A synthesis of recent work on the Red Pine Shale and related undivided clastic strata, northeastern Utah, US, *in* Link, P.K., and Lewis, R., eds., Proterozoic Basins of Northwestern US: Society for Sedimentary Geology Special Publication, v. 86, p. 151–166.

DeMaster, D.J., 1981, The supply and accumulation of silica in the marine environment: Geochimica et Cosmochimica Acta, v. 45, p. 1715–1732, https://doi.org/10.1016/0016-7037(81)90006-5.

Diffenbaugh, N.S., Ashfaq, M., Shuman, B., Williams, J.W., and Bartlein, P.J., 2006, Aridity in the United States: Response to mid-Holocene changes in insolation and sea surface temperature: Geophysical Research Letters, v. 33, L22712, https://doi.org/10.1029/2006GL028012.

Digerfeldt, G., 1986, Studies on past lake-level fluctuations, *in* Berglund, B.E., ed., Handbook of Holocene Palaeoecology and Palaeohydrology: Hoboken, New Jersey, USA, John Wiley & Sons, p. 127–143.

Douglass, D.C., 2000, Glacial history of the west fork of Beaver Creek, Uinta Mountains, Utah [M.S. thesis]: Madison, Wisconsin, USA, University of Wisconsin, 64 p.

Ebel, R., and Munroe, J.S., 2015, Colloidal sediment in the Uinta Range, Utah: The Green: The Mountain Geologist, v. 42, p. 7.

Fall, P.L., 1988, Vegetation dynamics in the southern Rocky Mountains: Late Pleistocene and Holocene timberline fluctuations [unpublished Ph.D. dissertation]: Tucson, Arizona, USA, University of Arizona.

Frechette, J.D., and Meyer, G.A., 2009, Holocene fire-related alluvial-fan deposition and climate in ponderosa pine and mixed-conifer forests, Sacramento Mountains, New Mexico, USA: The Holocene, v. 19, p. 639–651.

Gauthier, A., and Muñoz, A., 2009, Seasonal sedimentation in the Pliocene Villarroya Lake (N Spain) inferred from pollen analysis: Sedimentary Geology, v. 222, p. 111–123, https://doi.org/10.1016/j.sedgeo.2009.06.008.

Heiri, O., Lotter, A.F., and Lemcke, G., 2001, Loss on ignition as a method for estimating organic and carbonate content in sediments: Reproducibility and comparability of results: Journal of Paleolimnology, v. 25, p. 101–110, https://doi.org/10.1023/A:1008119611481.

Jacoby, G.C., 1975, An overview of the effect of Lake Powell on Colorado River Basin water supply and environment: Los Angeles, California, USA, Lake Powell Research Project.

Jeppson, R.W., Ashcroft, G.L., Huber, A.L., Skogerbee, G.V., and Bagley, J.M., 1968, Hydrologic atlas of Utah: Logan, Utah, USA, Utah Water Research Laboratory, Utah State University, 306.

Johnson, B.G., Jiménez-Moreno, G., Eppes, M.C., Diemer, J.A., and Stone, J.R., 2013, A multiproxy record of postglacial climate variability from a shallowing, 12-m deep sub-alpine bog in the southeastern San Juan Mountains of Colorado, USA: The Holocene, v. 23, p. 1028–1038.

Laabs, B.J.C., and Carson, E.C., 2005, Glacial geology of the southern Uinta Mountains, *in* Dehler, C.M., Pederson, J.L., Sprinkel, D.A., and Kowallis, B.J., eds., Uinta Mountain Geology: Utah Geological Association Publication 33, p. 235–253.

Laabs, B.J.C., Refsnider, K.A., Munroe, J.S., Mickelson, D.M., Applegate, P.J., Singer, B.S., and Caffee, M.W., 2009, Latest Pleistocene glacial chronology of the Uinta Mountains: Support for moisture-driven asynchrony of the last deglaciation: Quaternary Science Reviews, v. 28, p. 1171–1187, https://doi.org/10.1016/j.quascirev.2008.12.012.

Larsen, D.J., Finkenbinder, M.S., Abbott, M.B., and Ofstun, A.R., 2016, Deglaciation and postglacial environmental changes in the Teton Mountain Range recorded at Jenny Lake, Grand Teton National Park, WY: Quaternary Science Reviews, v. 138, p. 62–75, https://doi.org/10.1016/j.quascirev.2016.02.024.

Liu, X., Vandenberghe, J., An, Z., Li, Y., Jin, Z., Dong, J., and Sun, Y., 2016, Grain size of Lake Qinghai sediments: Implications for riverine input and Holocene monsoon variability: Palaeogeography, Palaeoclimatology, Palaeoecology, v. 449, p. 41–51, https://doi.org/10.1016/j.palaeo.2016.02.005.

Livingstone, D.A., 1955, A lightweight piston sampler for lake deposits: Ecology, v. 36, p. 137–139, https://doi.org/10.2307/1931439.

Lundeen, Z., Brunelle, A., Burns, S.J., Polyak, V., and Asmerom, Y., 2013, A speleothem record of Holocene paleoclimate from the northern Wasatch Mountains, southeast Idaho, USA: Quaternary International, v. 310, p. 83–95, https://doi.org/10.1016/j.quaint.2013.03.018.

MacDonald, G.M., Beukens, R.P., and Kieser, W.E., 1991, Radiocarbon dating of limnic sediments: A comparative analysis and discussion: Ecology, v. 72, p. 1150–1155, https://doi.org/10.2307/1940612.

MacDonald, G.M., and Tingstad, A.H., 2007, Recent and multicentennial precipitation variability and drought occurrence in the Uinta Mountains region, Utah: Arctic, Antarctic, and Alpine Research, v. 39, p. 549–555, https://doi.org/10.1657/1523-0430(06-070)[MACDONALD]2.0.CO;2.

Marcott, S.A., Shakun, J.D., Clark, P.U., and Mix, A.C., 2013, A reconstruction of regional and global temperature for the past 11,300 years: Science, v. 339, p. 1198–1201.

Marshall, J.D., Jones, R.T., Crowley, S.F., Oldfield, F., Nash, S., and Bedford, A., 2002, A high resolution Late-Glacial isotopic record from Hawes Water, Northwest England: Climatic oscillations: Calibration and comparison of palaeotemperature proxies: Palaeogeography, Palaeoclimatology, Palaeoecology, v. 185, p. 25–40, https://doi.org/10.1016/S0031-0182(02)00422-4.

Mayewski, P.A., Rohling, E.E., Stager, J.C., and Karlén, W., 2004, Holocene climate variability: Quaternary Research, v. 62, p. 243–255, https://doi.org/10.1016/j.yqres.2004.07.001.

Menounos, B., 1997, The water content of lake sediments and its relationship to other physical parameters: An alpine case study: The Holocene, v. 7, p. 207–212, https://doi.org/10.1177/095968369700700208.

Mensing, S.A., and Southon, J.R., 1999, A simple method to separate pollen for AMS radiocarbon dating and its application to lacustrine and marine sediments: Radiocarbon, v. 41, p. 1–8, https://doi.org/10.1017/S0033822200019287.

Metcalfe, S.E., Barron, J.A., and Davies, S.J., 2015, The Holocene history of the North American Monsoon: 'known knowns' and 'known unknowns' in understanding its spatial and temporal complexity: Quaternary Science Reviews, v. 120, p. 1–27, https://doi.org/10.1016/j.quascirev.2015.04.004.

Meyers, P.A., and Ishiwatari, R., 1993, Lacustrine organic geochemistry: An overview of indicators of organic matter sources and diagenesis in lake sediments: Organic Geochemistry, v. 20, p. 867–900, https://doi.org/10.1016/0146-6380(93)90100-P.

Meyers, P.A., and Ishiwatari, R., 1995, Organic matter accumulation records in lake sediments, *in* Lerman, A., Imboden, D.M., and Gat, J.R., eds., Physics and Chemistry of Lakes: Berlin, Heidelberg, Germany, Springer, p. 279–328, https://doi.org/10.1007/978-3-642-85132-2_10.

Millspaugh, S.H., Whitlock, C., and Bartlein, P.J., 2000, Variations in fire frequency and climate over the past 17 000 yr in central Yellowstone National Park: Geology, v. 28, p. 211–214, https://doi.org/10.1130/0091-7613(2000)28<211:VIFFAC>2.0.CO;2.

Mitchell, V.L., 1976, The regionalization of climate in the western United States: Journal of Applied Meteorology, v. 15, p. 920–927, https://doi.org/10.1175/1520-0450(1976)015<0920:TROCIT>2.0.CO;2.

Mock, C.J., 1996, Climatic controls and spatial variations of precipitation in the western United States: Journal of Climate, v. 9, p. 1111–1125, https://doi.org/10.1175/1520-0442(1996)009<1111:CCASVO>2.0.CO;2.

Moreno, A., González-Sampériz, P., Morellón, M., Valero-Garcés, B.L., and Fletcher, W.J., 2012, Northern Iberian abrupt climate change dynamics during the last glacial cycle: A view from lacustrine sediments: Quaternary Science Reviews, v. 36, p. 139–153, https://doi.org/10.1016/j.quascirev.2010.06.031.

Moser, K.A., and Kimball, J.P., 2009, A 19,000-year record of hydrologic and climatic change inferred from diatoms from Bear Lake, Utah and Idaho, *in* Rosenbaum, J.G., and Kaufman, D.S., eds., Paleoenvironments of Bear Lake, Utah and Idaho, and its catchment: Geological Society of America Special Paper 450, p. 229–246, https://doi.org/10.1130/2009.2450(10).

Moser, K.A., Mordecai, J.S., Reynolds, R.L., Rosenbaum, J.G., and Ketterer, M.E., 2010, Diatom changes in two Uinta mountain lakes, Utah, USA: Responses to anthropogenic and natural atmospheric inputs: Hydrobiologia, v. 648, p. 91–108, https://doi.org/10.1007/s10750-010-0145-7.

Mourier, B., Poulenard, J., Carcaillet, C., and Williamson, D., 2010, Soil evolution and subalpine ecosystem changes in the French Alps inferred from geochemical analysis of lacustrine sediments: Journal of Paleolimnology, v. 44, p. 571–587, https://doi.org/10.1007/s10933-010-9438-0.

Munroe, J.S., 2002, Timing of postglacial cirque reoccupation in the northern Uinta Mountains, northeastern Utah, USA: Arctic, Antarctic, and Alpine Research, v. 34, p. 38–48, https://doi.org/10.1080/15230430.2002.12003467.

Munroe, J.S., 2003, Holocene timberline and palaeoclimate of the northern Uinta Mountains, northeastern Utah, USA: The Holocene, v. 13, p. 175–185, https://doi.org/10.1191/0959683603hl600rp.

Munroe, J.S., 2005, Glacial geology of the northern Uinta Mountains, *in* Dehler, C.M., Pederson, J.L., Sprinkel, D.A., and Kowallis, B.J., eds., Uinta Mountain Geology: Utah Geological Survey 33, p. 215–234.

Munroe, J.S., 2006, Investigating the spatial distribution of summit flats in the Uinta Mountains of northeastern Utah, USA: Geomorphology, v. 75, p. 437–449, https://doi.org/10.1016/j.geomorph.2005.07.030.

Munroe, J.S., 2007a, Exploring relationships between watershed properties and Holocene loss-on-ignition records in high-elevation lakes, southern Uinta Mountains, Utah, U.S.A: Arctic, Antarctic, and Alpine Research, v. 39, p. 556–565.

Munroe, J.S., 2007b, Properties of alpine soils associated with well-developed sorted polygons in the Uinta Mountains, Utah, USA: Arctic, Antarctic, and Alpine Research, v. 39, p. 578–591.

Munroe, J.S., 2012, Physical, chemical, and thermal properties of soils across a forest-meadow ecotone in the Uinta Mountains, Northeastern Utah, USA: Arctic,

Antarctic, and Alpine Research, v. 44, p. 95–106, https://doi.org/10.1657/1938-4246-44.1.95.

Munroe, J.S., 2014, Properties of modern dust accumulating in the Uinta Mountains, Utah, USA, and implications for the regional dust system of the Rocky Mountains: Earth Surface Processes and Landforms, v. 39, p. 1979–1988, https://doi.org/10.1002/esp.3608.

Munroe, J.S., 2019, Hydrogeomorphic controls on Holocene lacustrine loss-on-ignition records: Journal of Paleolimnology, v. 61, p. 53–68, https://doi.org/10.1007/s10933-018-0044-x.

Munroe, J.S., and Laabs, B.J.C., 2009, Glacial Geologic Map of the Uinta Mountains Area, Utah and Wyoming: Utah Geological Survey Miscellaneous Publication 09-4DM, scale map.

Munroe, J.S., and Laabs, B.J., 2017, Combining radiocarbon and cosmogenic ages to constrain the timing of the last glacial-interglacial transition in the Uinta Mountains, Utah, USA: Geology, v. 45, p. 171–174, https://doi.org/10.1130/G38156.1.

Munroe, J.S., and Mickelson, D.M., 2002, Last Glacial Maximum equilibrium-line altitudes and paleoclimate, northern Uinta Mountains, Utah, U.S.A: Journal of Glaciology, v. 48, p. 257–266, https://doi.org/10.3189/172756502781831331.

Munroe, J., Laabs, B., Shakun, J., Singer, B., Mickelson, D., Refsnider, K., and Caffee, M., 2006, Latest Pleistocene advance of alpine glaciers in the southwestern Uinta Mountains, Utah, USA: Evidence for the influence of local moisture sources: Geology, v. 34, p. 841–844, https://doi.org/10.1130/G22681.1.

Munroe, J.S., Crocker, T.A., Giesche, A.M., Rahlson, L.E., Duran, L.T., Bigl, M.F., and Laabs, B.J.C., 2012, A lacustrine-based Neoglacial record for Glacier National Park, Montana, USA: Quaternary Science Reviews, v. 53, p. 39–54, https://doi.org/10.1016/j.quascirev.2012.08.005.

Munroe, J.S., Klem, C.M., and Bigl, M.F., 2013, A lacustrine sedimentary record of Holocene periglacial activity from the Uinta Mountains, Utah, U.S.A: Quaternary Research, v. 79, p. 101–109, https://doi.org/10.1016/j.yqres.2012.12.006.

Munroe, J.S., Attwood, E.C., O'Keefe, S.S., and Quackenbush, P.J., 2015, Eolian deposition in the alpine zone of the Uinta Mountains, Utah, USA: Catena, v. 124, p. 119–129, https://doi.org/10.1016/j.catena.2014.09.008.

Myer, C.A., 2008, Sedimentology, stratigraphy, and organic geochemistry of the Red Pine Shale, Uinta Mountains, Utah: A prograding deltaic system in a mid-Neoproterozoic interior seaway [M.A. thesis]: Logan, Utah, USA, Utah State University.

Neff, J.C., Ballantyne, A.P., Farmer, G.L., Mahowald, N.M., Conroy, J.L., Landry, C.C., Overpeck, J.T., Painter, T.H., Lawrence, C.R., and Reynolds, R.L., 2008, Increasing eolian dust deposition in the western United States linked to human activity: Nature Geoscience, v. 1, p. 189–195, https://doi.org/10.1038/ngeo133.

Noble, P.J., Ball, G.I., Zimmerman, S.H., Maloney, J., Smith, S.B., Kent, G., Adams, K.D., Karlin, R.E., and Driscoll, N., 2016, Holocene paleoclimate history of Fallen Leaf Lake, CA., from geochemistry and sedimentology of well-dated sediment cores: Quaternary Science Reviews, v. 131, part A, p. 193–210, https://doi.org/10.1016/j.quascirev.2015.10.037.

Noren, A.J., Bierman, P.R., Steig, E.J., Lini, A., and Southon, J., 2002, Millennial-scale storminess variability in the northeastern United States during the Holocene epoch: Nature, v. 419, p. 821–824, https://doi.org/10.1038/nature01132.

O'Keefe, S.S., McElroy, R., and Munroe, J.S., 2016a, Determining the Influence of Dust on Post-Glacial Lacustrine Sedimentation in Bald Lake, Uinta Mountains, Utah: Abstract A21E-0114 presented at AGU Fall Meeting, 12–16 December, San Francisco, California, USA.

O'Keefe, S.S., McElroy, R.C., and Munroe, J.S., 2016b, Using lake sediment records to reconstruct post-glacial dust delivery to high-elevation lakes in the Uinta Mountains, Utah: Geological Society of America Abstracts with Programs, v. 48, no.2, https://doi.org/10.1130/abs/2016NE-272206.

Parris, A.S., Bierman, P.R., Noren, A.J., Prins, M.A., and Lini, A., 2010, Holocene paleostorms identified by particle size signatures in lake sediments from the Northeastern United States: Journal of Paleolimnology, v. 43, p. 29–49, https://doi.org/10.1007/s10933-009-9311-1.

Power, M.J., Whitlock, C., and Bartlein, P.J., 2011, Postglacial fire, vegetation, and climate history across an elevational gradient in the Northern Rocky Mountains, USA and Canada: Quaternary Science Reviews, v. 30, p. 2520–2533, https://doi.org/10.1016/j.quascirev.2011.04.012.

Rasmussen, S.O., Andersen, K.K., Svensson, A., Steffensen, J.P., Vinther, B.M., Clausen, H.B., Siggaard-Andersen, M., Johnsen, S.J., Larsen, L.B., and Dahl-Jensen, D., 2006, A new Greenland ice core chronology for the last glacial termination: Journal of Geophysical Research. Atmospheres, v. 111, no. D6, https://doi.org/10.1029/2005JD006079.

Reasoner, M.A., 1993, Equipment and procedure improvements for a lightweight, inexpensive, percussion core sampling system: Journal of Paleolimnology, v. 8, p. 273–281, https://doi.org/10.1007/BF00177859.

Reasoner, M.A., and Jodry, M.A., 2000, Rapid response of alpine timberline vegetation to the Younger Dryas climate oscillation in the Colorado Rocky Mountains, USA: Geology, v. 28, p. 51–54, https://doi.org/10.1130/0091-7613(2000)28<51:RROATV>2.0.CO;2.

Refsnider, K.A., Laabs, B.J.C., Plummer, M.A., Mickelson, D.M., Singer, B.S., and Caffee, M.W., 2008, Last glacial maximum climate inferences from cosmogenic dating and glacier modeling of the western Uinta ice field, Uinta Mountains, Utah: Quaternary Research, v. 69, p. 130–144, https://doi.org/10.1016/j.yqres.2007.10.014.

Reimer, P.J., Bard, E., Bayliss, A., and Beck, J.W., 2013, IntCal13 and Marine13 radiocarbon age calibration curves 0–50,000 years cal BP: Radiocarbon, v. 55, p. 1869–1887, https://doi.org/10.2458/azu_js_rc.55.16947.

Ropelewski, C.F., Gutzler, D.S., Higgins, R.W., and Mechoso, C.R., 2005, The North American Monsoon System, *in* Chang, C.-P., Wang, B., and Lau, N.-C.G., eds., The Global Monsoon System: Research and Forecast: Report of the International Committee of the Third International Workshop on Monsoons (IWM-III), 2–6 November, 2004, Hangzhou, China, p. 207–218.

Routson, C.C., Overpeck, J.T., Woodhouse, C.A., and Kenney, W.F., 2016, Three millennia of southwestern North American dustiness and future implications: PLoS One, v. 11, e0149573, https://doi.org/10.1371/journal.pone.0149573.

Saros, J.E., Interlandi, S.J., Wolfe, A.P., and Engstrom, D.R., 2003, Recent changes in the diatom community structure of lakes in the Beartooth Mountain Range, U.S.A.: Arctic, Antarctic, and Alpine Research, v. 35, p. 18–23.

Sears, J., Graff, P., and Holden, G., 1982, Tectonic evolution of lower Proterozoic rocks, Uinta Mountains, Utah and Colorado: Geological Society of America Bulletin, v. 93, p. 990–997, https://doi.org/10.1130/0016-7606(1982)93<990:TEOLPR>2.0.CO;2.

Shaw, J.D., and Long, J.N., 2007, Forest ecology and biogeography of the Uinta Mountains, USA: Arctic, Antarctic, and Alpine Research, v. 39, p. 614–628.

Shuman, B., Bartlein, P.J., and Webb, T., III, 2005, The magnitudes of millennial-and orbital-scale climatic change in eastern North America during the Late Quaternary: Quaternary Science Reviews, v. 24, p. 2194–2206, https://doi.org/10.1016/j.quascirev.2005.03.018.

Shuman, B., Henderson, A.K., Colman, S.M., Stone, J.R., Fritz, S.C., Stevens, L.R., Power, M.J., and Whitlock, C., 2009, Holocene lake-level trends in the Rocky Mountains, USA: Quaternary Science Reviews, v. 28, p. 1861–1879, https://doi.org/10.1016/j.quascirev.2009.03.003.

Shuman, B., Pribyl, P., Minckley, T.A., and Shinker, J.J., 2010, Rapid hydrologic shifts and prolonged droughts in Rocky Mountain headwaters during the Holocene: Geophysical Research Letters, v. 37, no. 6, https://doi.org/10.1029/2009GL042196.

Shuman, B.N., and Serravezza, M., 2017, Patterns of hydroclimatic change in the Rocky Mountains and surrounding regions since the last glacial maximum: Quaternary Science Reviews, v. 173, p. 58–77, https://doi.org/10.1016/j.quascirev.2017.08.012.

Shuman, B.N., Pribyl, P., and Buettner, J., 2015, Hydrologic changes in Colorado during the mid-Holocene and Younger Dryas: Quaternary Research, v. 84, p. 187–199, https://doi.org/10.1016/j.yqres.2015.07.004.

Smoot, J.P., and Rosenbaum, J.G., 2009, Sedimentary constraints on late Quaternary lake-level fluctuations at Bear Lake, Utah and Idaho, *in* Rosenbaum, J.G., and Kaufman, D.S., eds., Paleoenvironments of Bear Lake, Utah and Idaho, and its catchment: Geological Society of America Special Paper 450, p. 263–290, https://doi.org/10.1130/2009.2450(12).

Stone, J.R., and Fritz, S.C., 2006, Multidecadal drought and Holocene climate instability in the Rocky Mountains: Geology, v. 34, p. 409–412, https://doi.org/10.1130/G22225.1.

Street, F.A., and Grove, A.T., 1979, Global maps of lake-level fluctuations since 30,000 yr BP: Quaternary Research, v. 12, p. 83–118, https://doi.org/10.1016/0033-5894(79)90092-9.

Strickland, J.D.H., and Parsons, T.R., 1965, A manual of sea water analysis, Ottawa: Fisheries Research Board of Canada, Bulletin 125, 203 p.

Vinther, B.M., Clausen, H.B., Johnsen, S.J., Rasmussen, S.O., Andersen, K.K., Buchardt, S.L., Dahl-Jensen, D., Seierstad, I.K., Siggaard-Andersen, M.-L., and Steffensen, J.P., 2006, A synchronized dating of three Greenland ice cores throughout the Holocene: Journal of Geophysical Research, Atmospheres, v. 111, no. D13, https://doi.org/10.1029/2005JD006921.

Wanner, H., Solomina, O., Grosjean, M., Ritz, S.P., and Jetel, M., 2011, Structure and origin of Holocene cold events: Quaternary Science Reviews, v. 30, p. 3109–3123, https://doi.org/10.1016/j.quascirev.2011.07.010.

Whitlock, C., and Bartlein, P.J., 1993, Spatial variations of Holocene climatic change in the Yellowstone region: Quaternary Research, v. 39, p. 231–238, https://doi.org/10.1006/qres.1993.1026.

Whitlock, C., and Larsen, C., 2002, Charcoal as a fire proxy, *in* Smol J.P., Birks H.J.B., Last W.M., Bradley R.S., and Alverson K., eds., Tracking Environmental Change Using Lake Sediments: Dordrecht, The Netherlands, Springer, p. 75–97, https://doi.org/10.1007/0-306-47668-1_5.

Wolfe, A.P., Van Gorp, A.C., and Baron, J.S., 2003, Recent ecological and biogeochemical changes in alpine lakes of Rocky Mountain National Park (Colorado, USA): A response to anthropogenic nitrogen deposition: Geobiology, v. 1, p. 153–168, https://doi.org/10.1046/j.1472-4669.2003.00012.x.

Xiao, J., Chang, Z., Si, B., Qin, X., Itoh, S., and Lomtatidze, Z., 2009, Partitioning of the grain-size components of Dali Lake core sediments: Evidence for lake-level changes during the Holocene: Journal of Paleolimnology, v. 42, p. 249–260, https://doi.org/10.1007/s10933-008-9274-7.

Yellen, B., Woodruff, J.D., Kratz, L.N., Mabee, S.B., Morrison, J., and Martini, A.M., 2014, Source, conveyance and fate of suspended sediments following Hurricane Irene. New England, USA: Geomorphology, v. 226, p. 124–134, https://doi.org/10.1016/j.geomorph.2014.07.028.

Zhao, Y., and Harrison, S.P., 2012, Mid-Holocene monsoons: A multi-model analysis of the inter-hemispheric differences in the responses to orbital forcing and ocean feedbacks: Climate Dynamics, v. 39, p. 1457–1487, https://doi.org/10.1007/s00382-011-1193-z.

Science Editor: Bradley S. Singer
Associate Editor: John Jansen

Manuscript Received 5 June 2018
Revised Manuscript Received 1 February 2019
Manuscript Accepted 21 March 2019

Printed in the USA